

PLATES

EXPLANATION PLATES I–XV

LEGEND TO ABBREVIATIONS USED IN PHOTOMICROGRAPHS

Ca	=	Calcite	
Do	=	Dolomite	
(Fe)Ca	=	Fe ²⁺ -poor ferroan calcite	
FeCa	=	Fe ²⁺ -rich ferroan calcite	
(Fe)Do	=	$\frac{\text{Fe}^{2+}}{\text{Mg}^{2+}} < 1$	} cf. Evamy (1963, 1969)
FeDo	=	$\frac{\text{Fe}^{2+}}{\text{Mg}^{2+}} > 1$	
DDo	=	Dedolomite (Evamy 1967)	
DrCa	=	Drusy Calcite	
ECa	=	Equant Calcite	
BlCa	=	Bladed Calcite	
DoRh	=	Rhombohedral dolomite crystal	
I	=	Intraclast	
V	=	Void	
F	=	Fracture	
S	=	Stylolite	
P	=	Pellet	
He	=	Hematite	
Qz	=	Quartz	
AQz	=	Authigenic Quartz	
R	=	Replacement	
mc	=	medium crystalline	} according to Bissell & Chilingar's (1967) modification of Wentworth's grade scale
fc	=	fine crystalline	
vfc	=	very fine crystalline	

Abbreviations in explanation as much as possible in brackets.
 Arrow indicates stratigraphic top. Locations of intervals pictured in field photographs, and of samples used for (electron) photomicrographs, are indicated on Enclosures I–IV.

Thin sections prepared by Mr. J. Schipper.
 Photomicrographs prepared by Mr. W. C. Laurijssen and Mr. W. A. M. Devilé. Electron microscope photographs by Mr. W. de Priester. Field photographs by the author.

PLATE I

I-1. Section 32. Base. Ooid bed in Veneros Member. Bedding 10-30 cm thick and slightly wavy. Yellowish grey (5 Y 8/1) or moderate orange pink (5 YR 8/1) weathering colours. Ooid bed is transitional between the brown sandy and silty lowermost beds (Sst) and the moderately grey packstones (Pst).

I-2. Section 29. Two metres from base. Ooid bed in Veneros Member. Grainstone with cross-stratification, gullies and graded beds. Grains are mainly crinoidal and bryozoan fragments. Colour is medium light grey (N 6).

I-3. Section 32. Sample 23. Stained with $K_3Fe(CN)_6$. Ooid facies. This oolite mainly contains coated grains and true (radial) ooids. The radially oriented enveloping crystals display a preference for sheltered areas (arrow). The nuclei are bioclasts (cf. Pl. I-4) or detrital quartz grains. Clear drusy vaguely blade-shaped calcite crystals (BICa), not containing any trace of ferroan calcite, are present around the ooids as a 'halo'. The remaining inter-ooid space is filled with equant medium calcite crystals mainly composed of ferroan calcite (ECa). Hematite patches (He), which especially replace parts of the enveloping layers of the nuclei, are irregularly distributed throughout the sample.

I-4. Section 32. Sample 23. Negative photomicrograph. Stained with alizarin red S and $K_3Fe(CN)_6$. Ooid facies. Bioclastic grains are mainly brachiopods, bryozoans (Cryptostomata; especially Fenestrata) and ostracods. Superficial ooids with radial coatings, coated grains and a few true ooids are present. Nuclei of the ooids are bioclasts and detrital quartz grains. Interstitial material (cf. Pl. I-3) is in some places pseudosparite. Moreover, clear drusy blade-shaped calcite crystals and equant medium ferroan calcite crystals are present. Fractures (F) cross the bioclasts. They are filled with (Fe)Ca cement. Sometimes the walls of the fractures are coated with films of hematite. Hematite patches (He) are irregularly distributed throughout the sample.

I-5. Section 17. Sample V-7. Stained with alizarin red S. Ooid facies. Two layers envelop crinoidal and quartz nuclei. Crinoidal nuclei consist mainly of (FeCa) with hematite impregnations in the pores. Quartz (cf. Pl. I-7) is partly replaced (R) by pellets and ooids and has, in some places, a somewhat corroded aspect. The orientation of the crystals in the envelopes around the nuclei is radial; their composition is (FeCa). There are rims containing much ferruginous material, and forming a dark 'halo' in the ooids (He). Intergranular material consists of equant medium (Fe)Ca crystals. No blade-shaped calcite crystals are present around the ooids. The periphery of the ooids and of the pellets (?) is irregular and is attacked by the cement. The intercrystalline boundaries of these cement crystals are straight.

I-6. Section 20. Sample 1. Stained with alizarin red S and $K_3Fe(CN)_6$. Ooid facies. Oolite consists of true ooids with bioclastic grains and detrital quartz grains as nuclei. The enveloping material consists of two layers; a radial and a concentric one. The latter is composed of various lamellae. The two layers are separated by a dark stylolitic (S) zone containing (He). Many pellets (?) (P) or transections through ooids not touching the nucleus are scattered throughout the thin section. The contacts between the pellets (?) and the ooids can be stylolitic (S) or microstylolitic (cf. Park & Schot, 1968), and serrated. Replacements occur (R). The composition of the enveloping material is (FeCa). The inter-ooid material is drusy calcite (DrCa). Tiny blade-shaped crystals coat the ooids and the pellets (?). The remaining space is filled with (Fe)Ca equant medium crystals and with a few scattered (FeDo) crystals. The lighter crystals are calcite; the darker ones are dolomite.

I-7. Section 17. Sample V-7. Stained with a mixture of alizarin red S and $K_3Fe(CN)_6$. Ooid facies. Oolite is composed of true ooids. Some ooids are irregular as a result of replacement processes (R). Bimodality in size is clearly visible. The enveloping crystals are radially oriented but some concentric lamellae are visible. The innermost layer is radial (quiet depositional conditions according to Rusnak, 1960); the outermost layer is concentric (higher turbulent conditions; Rusnak, 1960). The composition is (FeCa). Nuclei may be crinoidal fragments which are highly impregnated with hematitic material and which consist of (Fe)Ca-(FeCa) material. In the enveloping material, idiomorphic quartz is present. Interstitially equant medium (Fe)Ca crystals are present. Some fractures (F) cross the ooids.

I-8. Section 24. Sample 559. Stained with a mixture of alizarin red S and $K_3Fe(CN)_6$. Ooid facies. Oolite containing radial true ooids composed of (FeCa). The inter-ooid space is filled with patchy anhedral (FeDo) and (Do) crystals, and with some (DoRh) crystals composed of (FeDo) and coated with ferruginous material. Patches of pure (Do) are present, both in the (DoRh) in locations where no coatings occur and in the inter-ooid cement. Crystals of the cement form a mosaic-like interlocking system. The nucleus of one ooid is an idiomorphic quartz crystal (Qz). Arrows indicate (Do) patchy crystals.

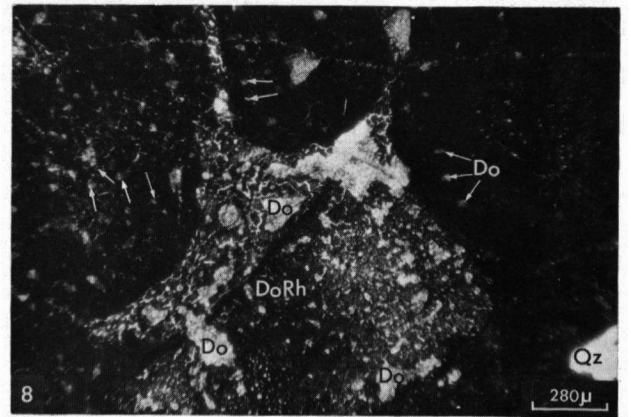
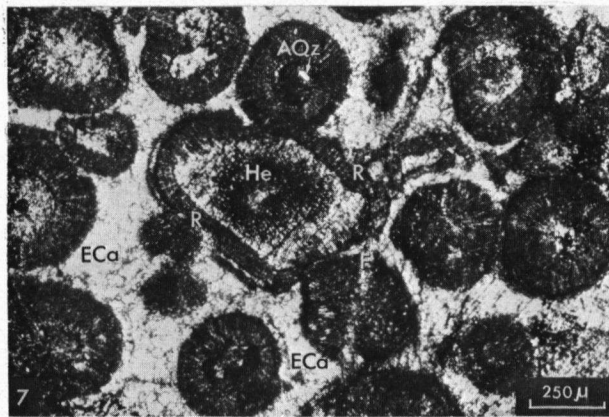
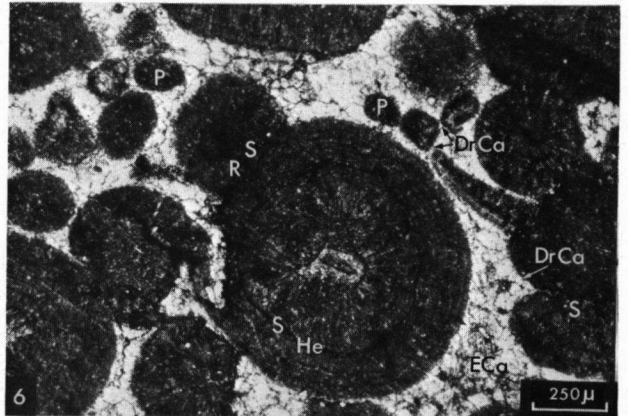
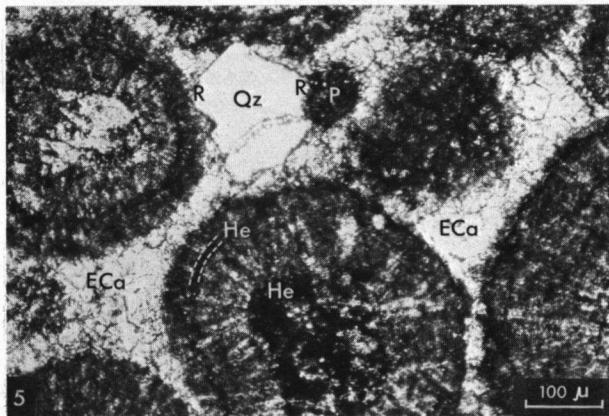
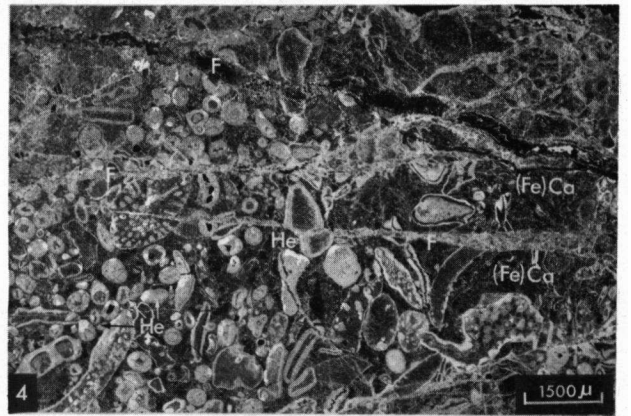
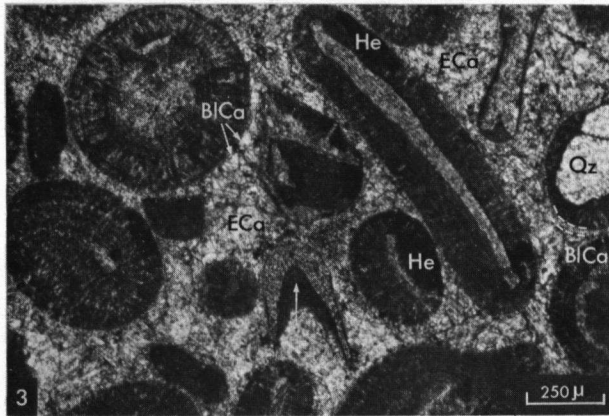
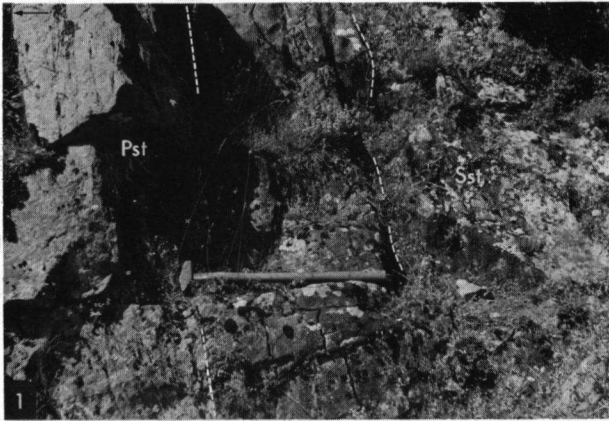


PLATE II

II-1. Section 9. Eighteen metres from the base. Facies e. Medium grey, medium bedded layers alternating with thin bedded layers. The contacts between the layers are stylolitic. The depositional texture is mainly packstone (Pst) and grainstone (Gst). Only crinoidal ossicles can be recognized when using a hand lens. The thin-layered beds contain some chert. Between the grainstone-packstone beds, argillaceous material (A) is intercalated in layers. In the grainstone and packstone beds the effect of recrystallization is moderate to strong.

II-2. Section 33. Four metres from base at the transition from the Veneros Member to Member B. Facies f and g. Shaly and marly material (Sh) intercalated in between bioclastic packstones (Pst). In the shales and marls, large (up to 15 cm) zaphrentoid solitary rugose (Z) corals and platy tabulate corals (Pl) are present. The intercalating siliciclastic layers are 20-50 cm thick.

II-3. Section 28. Base. Facies f-g. A slightly recrystallized packstone-grainstone (Pst-Gst) containing crinoids, bryozoans and brachiopods. Bedding is medium (up to 30 cm). Pinkish grey (5 YR 8/1) recrystallization patches (Pa) in the limestones are characteristic. The regular medium-bedded parts alternate with argillaceous layers up to 50 cm thick and contain platy tabulate corals and solitary zaphrentoid rugose corals (cf. Pl. II-2). In these argillaceous layers important bryozoan and brachiopodal faunas could be collected (cf. Pl. II-8).

II-4. Section 28. Four metres from the base. Facies f. Cross-bedding in a weathered packstone-grainstone (Pst-Gst) with crinoidal ossicles and fragments of bryozoans (e.g. Cyclostomata). Grading (finding upwards) is clearly visible. Gullies and pinchings-out are common. *Alveolites* sp. occurs in these beds.

II-5. Section 30. Approximately 6.50 m from base. Facies g. A regular alternation of irregular medium-layered packstone/grainstone beds (Pst-Gst) and siliciclastic (Sh) interbedded material. The depositional texture of the beds sometimes even grades into that of wackestone. The faunal elements in the pronounced grainstone-packstone-wackestone beds are crinoid ossicles and bryozoans (Cyclostomata and *Fenestella*), whereas in the interbedded argillaceous material solitary zaphrentoid rugose corals, branching and massive tabulate corals, gastropods, ostracods, styliolinas and trilobites are present.

II-6. Section 6. Three metres from base. Facies g. Enormous amounts of ramose tabulate corals (*Thamnopora* sp.) and platy tabulate corals (*Coenites* sp. and *Alveolites* sp.) are present in argillaceous greenish material. Brachiopods, too, were found. Bedding is not visible. The ramose fragments of the tabulate corals show a vague orientation.

II-7. Section 29. Ten metres from base. Facies g. A packstone-grainstone (Pst-Gst), mainly containing crinoidal ossicles and bryozoan fragments and showing small gullies filled with argillaceous material (A). Pinchings-out are visible. Siliciclastic material accentuates sedimentary structures.

II-8. Section 28. Base. Facies f-g. Argillaceous layer in between packstone-grainstone limestone (cf. Pl. II-3). Note the trapping of the fine-grained material by the fan-shaped bryozoans. The following faunal elements could be determined by Dr. Th. F. Krans (1969). Bryozoans: *Fenestella*, *Loculipora*, *Anastomopora* and *Lyropora*; Brachiopods: *Stropheodonta*, *Leptaena*, *Douvillina*, *Athyris*, *Cyrtina*, *Atrypa*, *Spinocyrtia*.

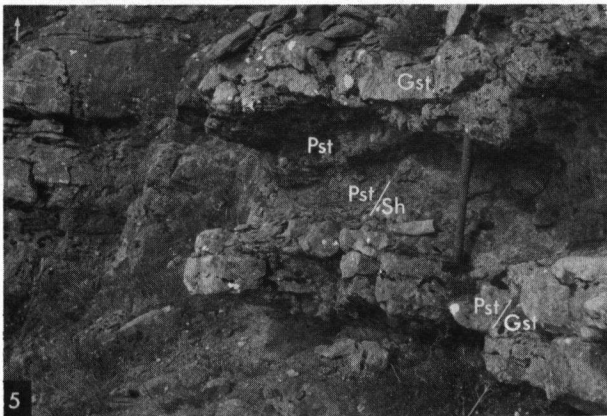
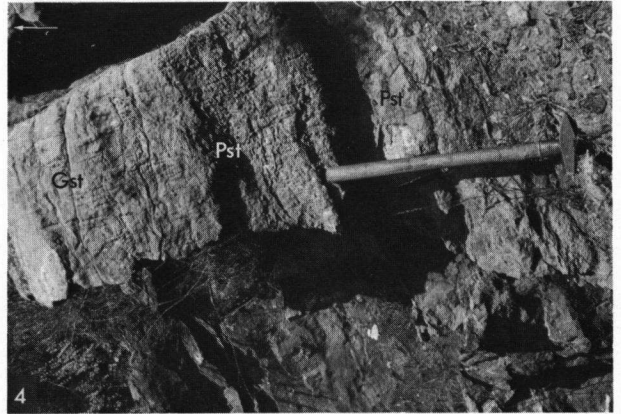
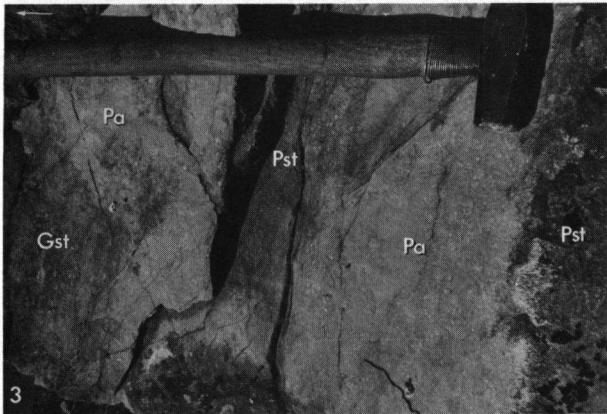
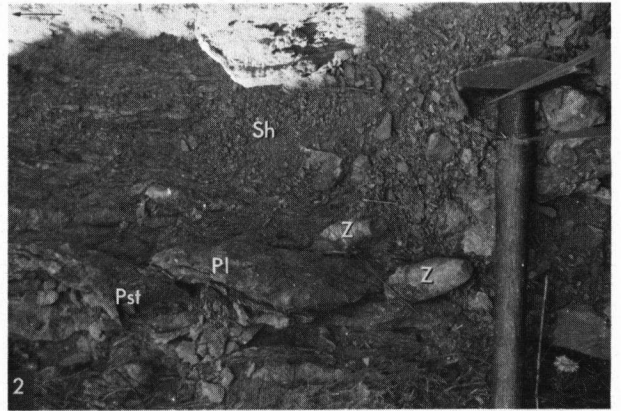


PLATE III

III-1. Section 4. Sample 432. Negative photomicrograph. Facies e. Not stained. This is a fairly well sorted encrinal calcarenite. The grains are mainly crinoidal. A number of bryozoans, ostracods and fragments of brachiopods and trilobites are present. Detrital, well-rounded quartz grains are present, mainly concentrated in stylolites (S). The stylolites are of the pressure solution type, since they cross and dissolve bioclasts. The interstitial material is sparry calcite. Crinoidal fragments show almost uniformly calcitic syntaxial cement rims. The remaining interstitial space is filled with (Fe)Do cement.

III-2. Section 4. Sample 434. Negative photomicrograph. Facies e. Not stained. This is a well-sorted encrinic calcarenite. Grains are mainly crinoidal with some ostracods and a few fragments of bryozoans. The intergranular material is mainly sparry calcite, present in the form of syntaxial calcite cement rims. Minor quantities of (Fe)Do are present. This cement was presumably introduced via fractures. Recrystallization moderately affected the rock. The planar crystal boundaries often cut the bioclasts and the former crystal boundaries. Some microstylolites of the pressure solution type are present.

III-3. Section 28. Sample 40. Negative photomicrograph. Stained with a mixture of alizarin red S and $K_3Fe(CN)_6$. Facies f. Regularly alternating pelletoid bioclastic calcarenite in which fine pellets are present, concentrated in layers (P), while in other layers cemented bioclasts (CBc) occur in abundance. At least two different types of bryozoans occur, as well as crinoids, brachiopods, trilobites and ostracods. One type of the bryozoans (Cryptostomate ?) encrusts the fine pelletoidal sediment, trapping it. Sheltering (the 'umbrella effect') produced voids that were subsequently filled with purely calcitic blade-shaped rimming crystals and finally with ferroan calcitic and some dolomitic equant blocky cement crystals. Depositional texture is grainstone to boundstone.

III-4. Section 33. Sample 2. Stained with a mixture of alizarin red S and $K_3Fe(CN)_6$. Facies f. The vague outlines of a tube produced by burrowing organisms are visible. In this tube an extremely large quantity of ferruginous material and of fine to very fine siliciclastic material is present. Some fragments of bioclasts are still recognizable (e.g. Fenestrata). The greatest amount, however, is diminished in size. The tube is present in a grainstone, composed of crinoid debris, brachiopodal fragments, bryozoans and ostracods. The cement in this surrounding material, presumably neomorphic pseudosparite, is (Fe)Ca in composition. Patchy dolomite and partly dissolved dolomite rhombohedral crystals are present.

III-5. Section 28. Sample 43. Negative photomicrograph. Not stained. Facies f. A strongly recrystallized packstone-grainstone mainly containing bryozoans, crinoids, ostracods, fragments of brachiopods and undeterminable bioclastic debris is crossed by solution stringers (S) in which ferruginous material is present. Rather significant quantities of detrital fine -sand -sized quartz and some detrital glauconite grains are present, mainly in the 'bands' formed by the solution stringers. Due to these 'bands', recrystallization results in a 'patchy' rock. These 'bands' are presumably produced by pressure which also can be the cause of the recrystallization (aggrading neomorphic process, Folk, 1965).

III-6. Section 30. Sample 241. Crossed nicols. Green monochromatic filter. Stained with a mixture of alizarin red S and $K_3Fe(CN)_6$. Facies f. In this packstone with bioclastic fragments (crinoid ossicles, ostracods, at least two different types of bryozoans) we also find authigenic quartz crystals (AQz) with idiomorphic shapes. In a few locations these idiomorphic authigenic quartz crystals are replaced by (Fe)Ca (cf. Pl. VI-4). Authigenesis of quartz can be proved with inclusions of the replaced material in the quartz crystals. The rock is crossed by fractures filled with (Fe)Ca cement (not visible). Idiomorphic authigenic quartz crystals are especially present near these fractures. Moreover, we find patches of subhedral to rhombohedral dolomite crystals (SDo). The dolomite crystals are formed after the formation of the fractures, since they cross these fractures. Dolomite also postdates the calcitic syntaxial grain growth rims of the crinoids. The remaining cement is composed of fine (Fe)Ca crystals (f).

III-7. Section 11. Sample 3. Stained with a mixture of alizarin red S and $K_3Fe(CN)_6$. Facies f. In this dolomitized coarse calcarenite with various fossil fragments (not visible in this photomicrograph) we find patchy dolomite and dolomite, pseudomorphic after authigenic (?) idiomorphic quartz (Pm). Some (DoRh) are also present, scattered throughout the sample. A process that can be imagined is the replacement of quartz by calcite (cf. Pl. VI-4), and subsequent replacement of this calcite by dolomite.

III-8. Section 28. Sample 44. Negative photomicrograph. Partly stained with alizarin red S and $K_3Fe(CN)_6$. Facies g. Well-rounded to fairly well-rounded quartz grains and a few detrital tourmaline grains are characteristic. Poorly sorted bioclastic debris, mainly of bryozoans, brachiopods and crinoids, also occur. Some pellets are present. A considerable amount of very fine detrital siliciclastic material and ferruginous matter, present interstitially, is characteristic. Cement is mainly (Fe)Ca. There is hardly any bioturbation in this thin section, though it is common in this rock type. We are here confronted with an argillaceous packstone containing silt-sized quartz grains.

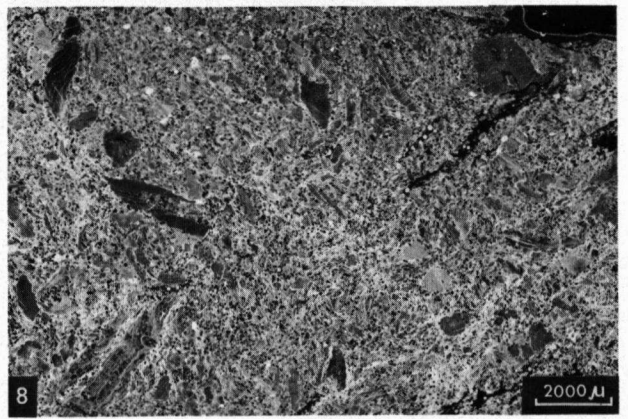
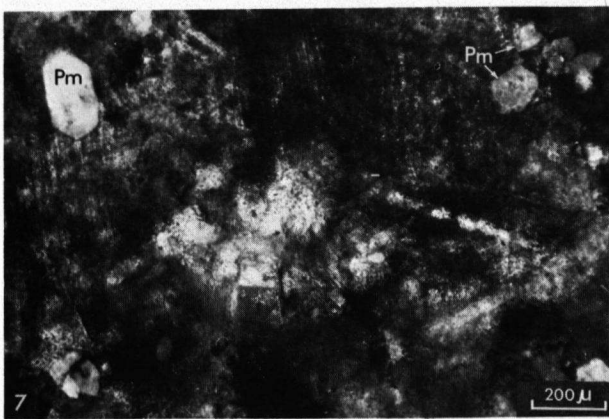
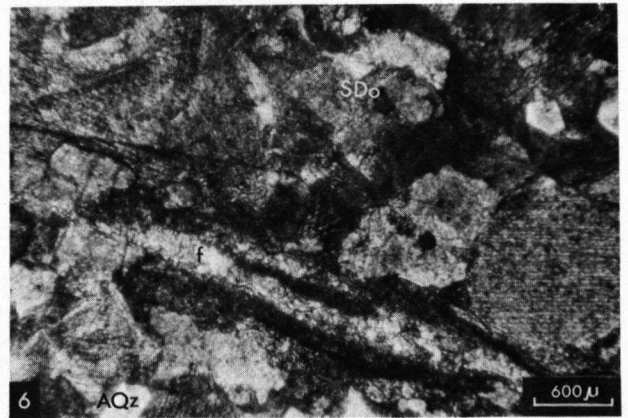
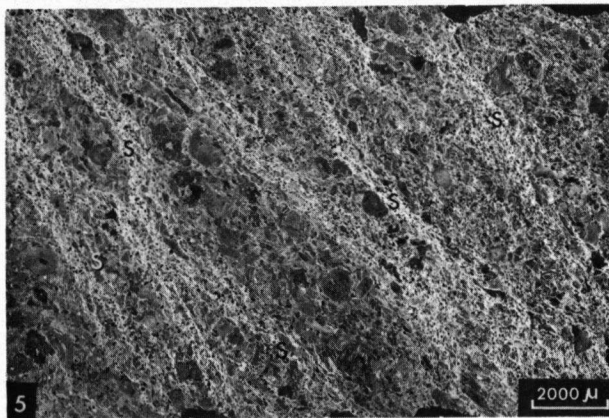
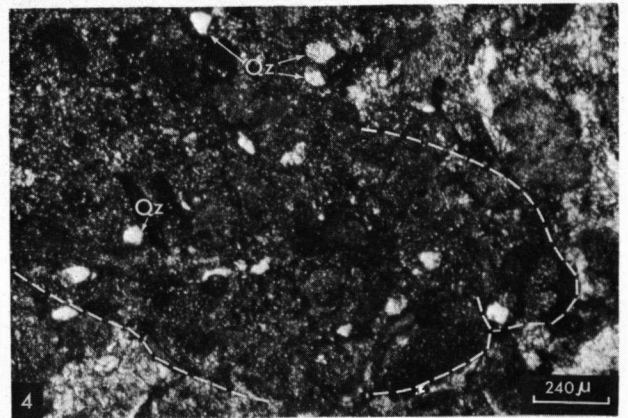
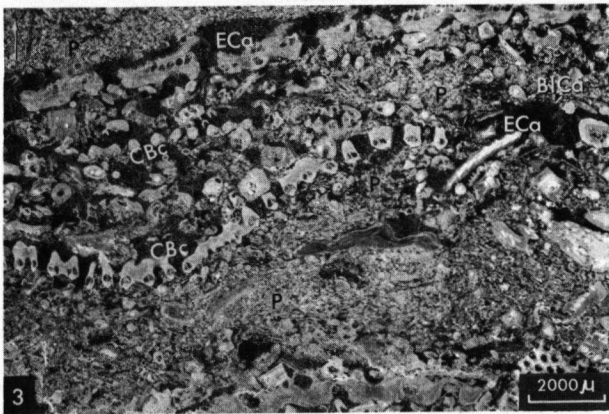
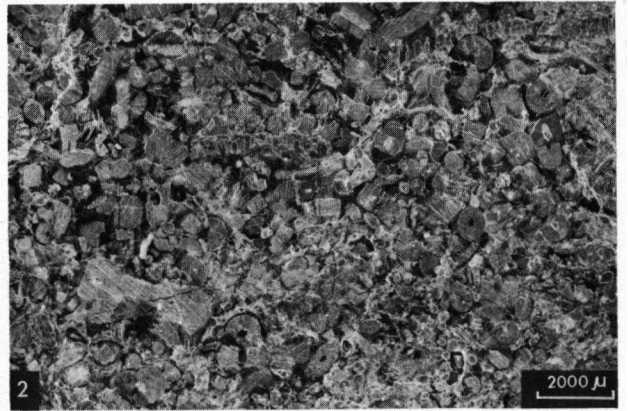
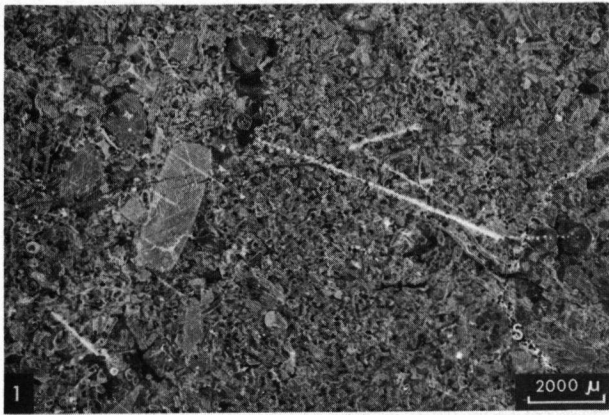


PLATE IV

IV-1 & 2. Section 31. Sample 149. Stained with a mixture of alizarin red S and $K_3Fe(CN)_6$. Facies f. This oolite consists of normal (true) ooids with enveloping layers consisting mainly of (FeCa) crystals. The crystals have a radial structure, although concentric lamellae are visible. Radial fibres are often composed of subhedral to anhedral secondary dolomite crystals (Fe)Do. Nuclei can be bioclastic fragments (degrading neomorphism) diminished in size, or hematitic (He) clotty aggregates. The radial arrangement of the crystals in the enveloping layer possibly indicates slow precipitation under moderately turbulent conditions (Rusnak, 1960). The inter-oid material is primarily an extremely small layer of blade-shaped rimming cement crystals (BlCa) around most of the ooids, followed by a mosaic of fine to very fine blocky equant ferroan calcitic crystals with straight intercrystalline boundaries, which fill the remaining space. Cracks (F) filled with Ca(Fe) cross the rocks.

IV-3. Section 26. Three metres from the base. Facies b. Medium grey (N 5) to medium light grey (N 6) well-layered beds with somewhat stylolitic and wavy contacts. Compound rugose corals and zaphrentoid rugose corals are present. Bioturbation is common. The appearance of the layers may be slightly nodular (N) (cf. Pl. IX-1).

IV-4. Section 18. Twenty-four to twenty-eight metres from the base. Facies c. Medium to thick-bedded sequence with gullies in which fining upwards sequences are present. Pinchings-out are common and occur laterally over 3-5 m. Some layers are thick, when primary bedding is obscured by recrystallization. Stylolites then give a rough indication of the primary depositional directions (cf. Pl. IX-2).

IV-5. Section 28. Twenty-five metres from the base. Facies c. Dark grey (N 3) to black (N 1) splintery, shale-like, often bituminous carbonate material, containing pyrite. Zaphrentoid rugose corals (Z) are sometimes present in great quantities. A fairly large amount of siliciclastic material (Sh) can be interbedded.

IV-6. Section 28. Twenty-four metres from the base. Facies c. Greyish black to black argillaceous material containing splintery limestone with *Alveolites* sp. (240 cm width) (Pl). Zaphrentoid rugose corals (Z) are also present.

IV-7. Section 7. Two metres from the base. Facies c. Very irregularly bedded sequence containing enormous quantities of bio clastic debris, mainly from platy (Pl) and from ramose (Ra) tabulate corals (e.g. *Alveolites* sp., *Coenites* sp., *Thamnopora* sp.). In the debris a depositional orientation is vaguely visible.

IV-8. Section 9. Ten metres from the base. Facies c. Bedding is irregular. We find an alternation of medium grey (N 5) packstones (Pst) with grainstones (Gst) and argillaceous limestones (A). The latter contain an abundance of compound rugose corals (C), ramose tabulate corals and platy tabulate corals. The massive bedded layers display 'loading' structures (L). The argillaceous material is clearly deposited around massive blocks of corals.

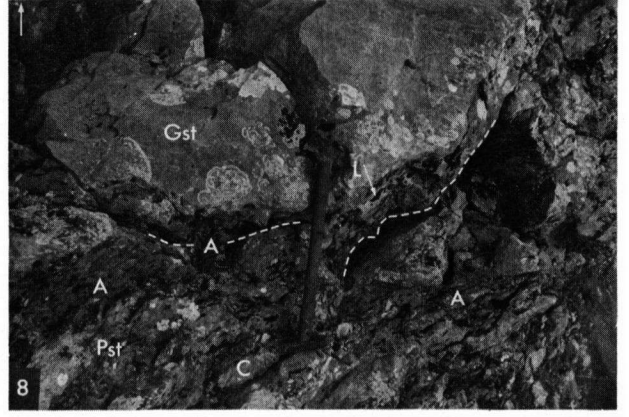
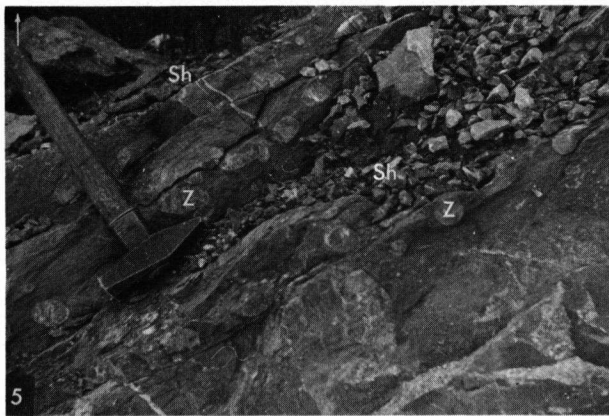
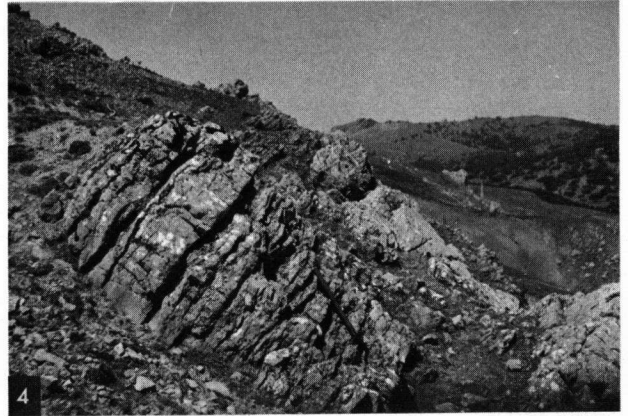
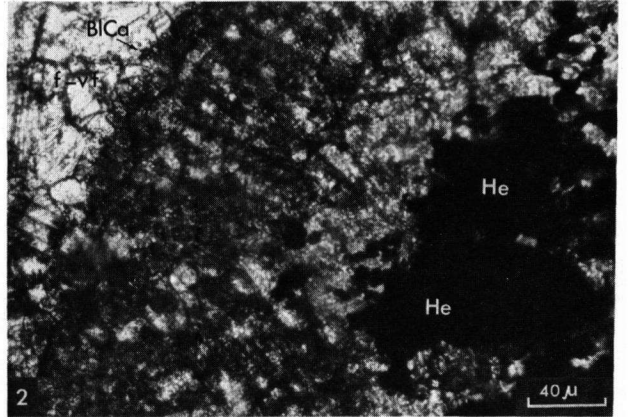
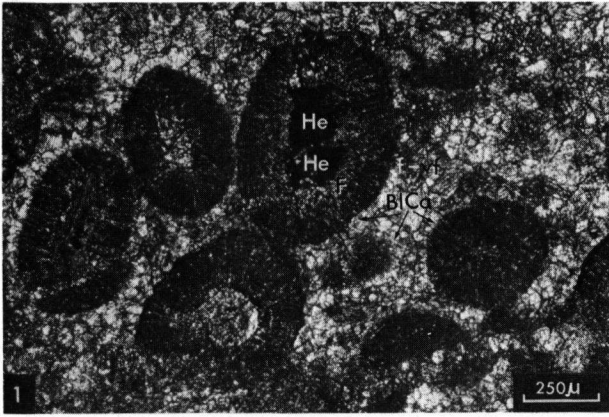


PLATE V

V-1. Section 33. Nine metres from the base. Facies f. Indurated bioclastic breccias, mainly from zaphrentoid rugose corals, compound rugose corals, ramose bryozoans, crinoidal debris and ramose tabulate corals, constitute the very irregular beds. The limestone is argillaceous, due to the large amount of siliciclastic material that is interbedded and admixed. Some lenticles containing less siliciclastic material are more resistant to weathering (L). A few corals were found in growth position. The colour of this limestone is medium dark grey (N 4).

V-2. Section 4. Sample 440. Negative photomicrograph. Stained with a mixture of alizarin red S and $K_3Fe(CN)_6$. Facies b. In this pelletaloid, very fine calcarenite we find enormous quantities of pellets. They have a vague, structureless ovoid shape. In addition, fragments of brachiopods, crinoids, trilobites, calcispheres and ostracods can be distinguished. Finally, there are a number of hematite clusters, and some indetermined ore is present. The cementing interstitial material is very fine crystalline calcite. In the vicinity of the numerous cracks ferroan dolomite and pure dolomite are distinguished. Some corroded (DoRh) are present. The rock is moderately attacked by recrystallization. Bioturbation is common.

V-3. Section 28. Sample 55. Negative photomicrograph. Stained with a mixture of alizarin red S and $K_3Fe(CN)_6$. Facies b. Large transported fragments of bioclasts, aulopore corals (?), crinoids, bryozoans and brachiopods are present in this wackestone. Interstitial material is very fine (disintegrated) bioclastic material. Many fractures (F) cross the sample. There are at least two generations, filled with cement. Contact between bioclasts and ground mass is generally stylolitic. Some vugs (V) are present. They are presumably of primary origin (arrow indicates top). They have basal sediments with hematite pellets and micritic matter. This material grows thinner towards the walls, which indicates that the introduction occurred late and mechanically. The remaining space is primarily filled with blade-shaped calcite crystals, rimming the walls, and in the centre we find medium equant calcite crystals. In the latter remains of fenestrate bryozoans are found, (not visible on this photomicrograph) the zoecia of which are filled with micritic material and silt.

V-4. Section 3. Sample 397. Negative photomicrograph. Stained with a mixture of alizarin red S and $K_3Fe(CN)_6$. Facies b. In this wackestone we find bioclastic particles, mainly fragments of stromatopores, ostracods, brachiopods, crinoids, calcispheres and some styliolinas. Pellets, too, are present. The interstitial material is micrite, sometimes consisting of disintegrated bioclastic matter. In the ground mass patches are present of medium equant calcite crystals (ECa) with straight intercrystalline boundaries. The cement in these patches is in direct irregular contact with the siltite-lutite ground mass. Some fractures are also present in this sample.

V-5. Section 30. Sample 244. Negative photomicrograph. Stained with a mixture of alizarin red S and $K_3Fe(CN)_6$. Facies b. In this strongly recrystallized rock type we distinguish vaguely crinoidal fragments and ostracods. The originally deposited matter was presumably mud and disintegrated bioclastic matter. Recrystallization and especially dolomitization have strongly attacked this rock. Dolomite is present in the form of (DoRh) crystals with ferroan dolomitic zones. Microstylolites, too, are present and partly filled with ferruginous material.

V-6. Section 4. Sample 439. Stained with a mixture of alizarin red S and $K_3Fe(CN)_6$. Facies f. A very fine grained packstone, mainly consisting of pellets (P). Some fragments of calcispheres and of ostracods, too, can be distinguished. The interstitial material is predominantly micrite, with some pseudosparitic patches. In some calcispheres blade-shaped calcite crystals are present. In this thin section a tube (T), made by a burrowing scavenger, is cut longitudinally. The tube is filled with dusty blade-shaped calcite crystals. In the walls of the tube a clearly distinguishable lineation (L) produced by the locomotion of the organism is visible, while the sediment in the host rock in direct contact with the lineated wall of the tube, shows signs of dragging (D). A few fractures (F) postdate the burrow tube. The rock is slightly recrystallized.

V-7. Section 30. Sample 244. Negative photomicrograph. Partly stained with a mixture of alizarin red S and $K_3Fe(CN)_6$. Facies c. In this vaguely layered coarse to medium calcarenite we find fragments of corals, of crinoids, of at least two different types of bryozoans, of brachiopods and of much undeterminable bioclastic debris. Pellets (P) are also present in great quantities. They occur mainly in places sheltered by means of the umbrella effect. In these places we also find voids (V) filled with zoned medium to coarse equant calcite and dolomite crystals. The zones in the dolomite crystals are alternations of (Do), (Fe)Do and (FeDo). The entire rock is moderately recrystallized. Some fractures are present.

V-8. Section 17. Sample IV-6. Stained with a mixture of alizarin red S and $K_3Fe(CN)_6$. Facies c. The general size of the bioclastic debris in this biosparite is medium. Some larger fragments are present. Sorting and roundness are moderate. Some pellets are present. The interstitial material was originally mud and very finely disintegrated bioclastic material. Recrystallization converted this into pseudosparite. Ghosts of the original bioclastic fragments and especially of the pellets are vaguely visible. Irregularly distributed patchy dolomite crystals (Do) occur in the cement. One rhombohedral pore is present, partly filled by dolomite, partly (along the surface) replaced by fine to very fine calcite.

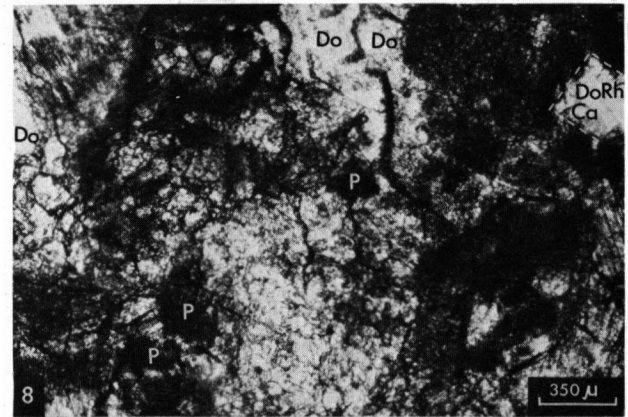
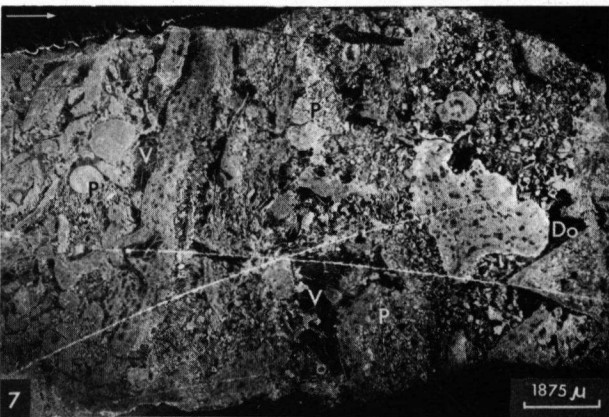
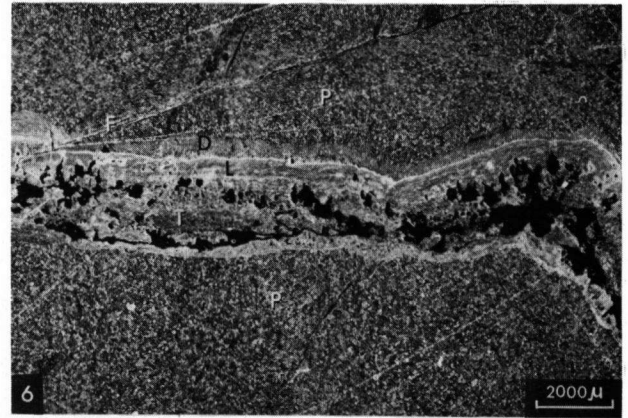
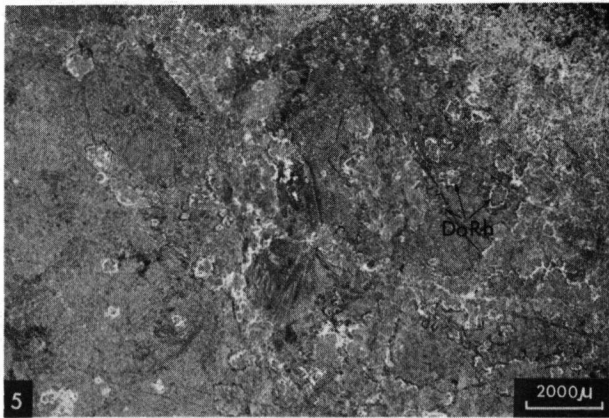
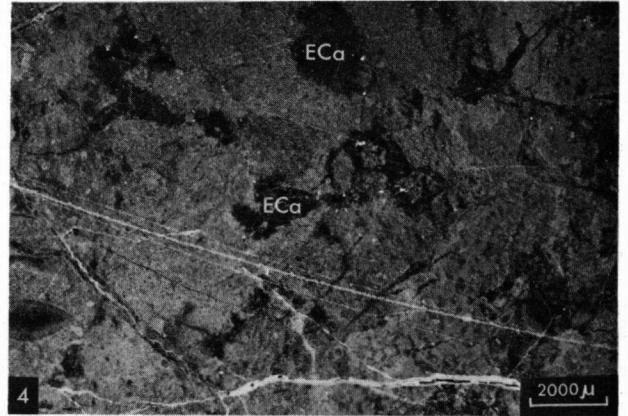
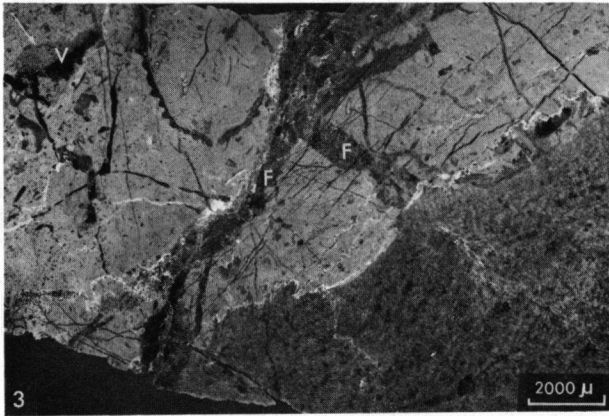
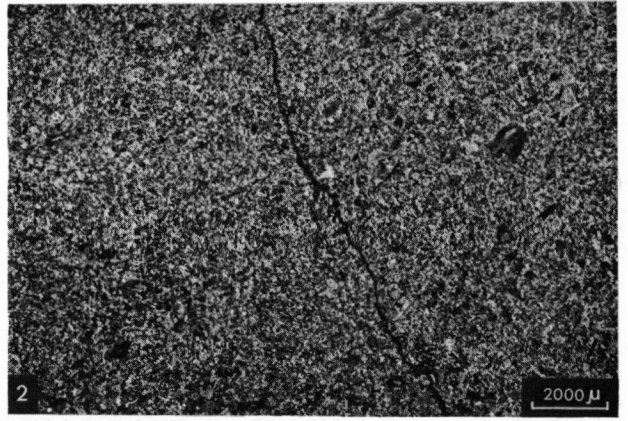
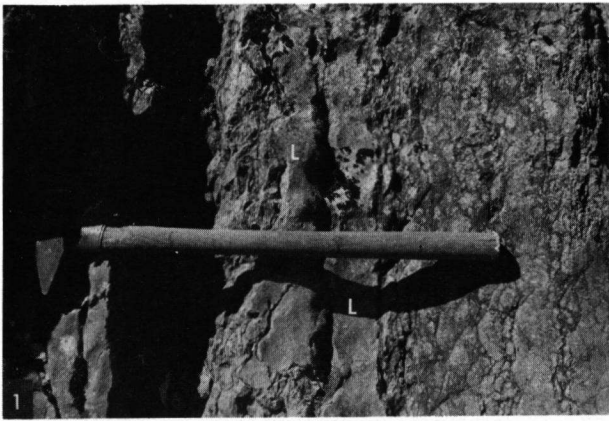


PLATE VI

VI-1. Section 17. Sample IV-6. Stained with a mixture of alizarin red S and $K_3Fe(CN)_6$. Facies c. Biosparite. The general size of the bioclastic fragments is medium. Some larger fragments are present. Solitary rugose corals, ramose tabulate corals, bryozoans, crinoidal fragments and ostracods can be distinguished. Sorting and roundness are moderate. Some pellets are present.

VI-2. Section 20. Sample 6. Stained with a mixture of alizarin red S and $K_3Fe(CN)_6$. Packstone-boundstone. This part of the photomicrograph shows a compound tabulate coral the calices of which are filled with drusy blade-shaped (BiCa) ferroan calcitic (FeCa) crystals, rimming the walls, and equant crystals in the centres.

VI-3. Section 16. Sample 14. Stained with a mixture of alizarin red S and $K_3Fe(CN)_6$. Facies c. Biosparite. Packstone. Recognizable fragments of tabulate corals, stromatoporoids, crinoids, brachiopods and bryozoans. The occurrence of many stylolites (S) and microstylolites, filled with opaque ore-fragments (presumably hematite), is typical. They cross bioclasts, dissolving them. Presumably they are of the pressure solution type. In the immediate vicinity of these stylolites, dark brown patches are present in which vaguely rhombohedral forms are visible. These patches are interpreted as hematite coated, partly replaced (DoRh). The cement is calcite, containing tiny patches of hematite and of ferruginous material.

VI-4. Section 24. Sample 568. Stained with a mixture of alizarin red S and $K_3Fe(CN)_6$. Facies c. In this biosparudite we mainly find crinoids and bryozoans. Pellets (P) are present as ghosts. Idiomorphic authigenic quartz grains are very common. The interstitial material is sparite and pseudosparite. The crinoidal fragments have syntaxial replacement rims. Many stylolites (S) cross the rock. Along the stylolites solution phenomena are visible. The authigenic idiomorphic quartz grains (AQz) are crossed by many minute cracks which give the quartz a mosaic like appearance. The crystals are often replaced in a patchy manner. They are always coated by a film of hematite (He). Replacement of the quartz by the calcite begins where the hematite layer is absent. That side is always close to a stylolite. Extension of the unreplaced quartz is straight. The rock is moderately attacked by recrystallization.

VI-5. Section 26. Sample 81. Negative photomicrograph. Stained with a mixture of alizarin red S and $K_3Fe(CN)_6$. Facies c. The following components are present in this packstone to wackestone; at least two types of bryozoans, ostracods, brachiopods, pelecypods and presumably gastropods. The interstitial material is very finely disintegrated bioclastic material. Sometimes it is micrite. In a few cases the larger bioclastic fragments cause primary voids (V₁) by means of the 'umbrella effect'. The contacts between the bioclasts and the ground mass are mainly stylolitic (S). The stylolites are filled with ferruginous material, concentrated via the fusion process of plane-parallel pressure solution surfaces of a zone by means of solution of the soluble beds in between these surfaces (Trurnit, 1968, p. 82). The primary voids are filled with equant medium to coarse calcite crystals. A few euhedral to subhedral dolomite crystals are present, scattered throughout the ground mass. Anhedronal dolomite patches were also observed. Geopetal fillings in zoecia indicate stratigraphic top (arrow). Microslumping phenomena are present (not visible in this photomicrograph). Burrowing is common. Due to numerous stylolites the appearance is somewhat breccia-like.

VI-6. Section 26. Sample 80. Negative photomicrograph. Stained with alizarin red S and $K_3Fe(CN)_6$. Facies c. In this packstone we recognize brachiopods, various types of bryozoans, crinoids, gastropods and ostracods as bioclastic fragments and, in addition, large amounts of pellets (P). The interstitial material is micritic and very fine-grained bioclastic material. The appearance of the sample is breccia-like, due to the many fractures (F) and stylolites (S). The broken fragments of the host rock resemble intraclasts (I). A few bioclasts have replacement rims (RR). The primary fossil voids (V₁) are filled with medium equant calcite; in a few cases the walls are rimmed with blade-shaped calcite crystals. Dolomite is present mainly as patches of anhedronal crystals. Sometimes cement patches are composed of (Fe)Do.

VI-7. Section 28. Sample 48. Stained with alizarin red S and $K_3Fe(CN)_6$. Facies c. In this packstone to boundstone we find ramose and compound tabulate corals, compound rugose corals, aulopore corals, gastropods, ostracods, bryozoans, brachiopods and crinoids (only partly visible). The interstitial material is mainly disintegrated bioclastic material and mud. In a few places (Fe)Ca cement is present. Geopetal structures are visible. In the ground mass a large quantity of hematitic material is present. A number of (DoRh) crystals coated with hematite are present. In many places the calcite cement is pseudosparite (PS).

VI-8. Section 27. Sample 196. Stained with a mixture of alizarin red S and $K_3Fe(CN)_6$. Facies c. In this grainstone we distinguish various types of bryozoans, crinoids and corals (partly visible). The interstitial material is sparry calcite. The sample is crossed by a number of stylolites that are filled with detrital ore; mainly hematite (He). This hematite is strongly clustered in stylolites and in micro-cracks, but does not influence the surroundings. The cement is composed of pure medium to fine (Ca) crystals (m-f, f).

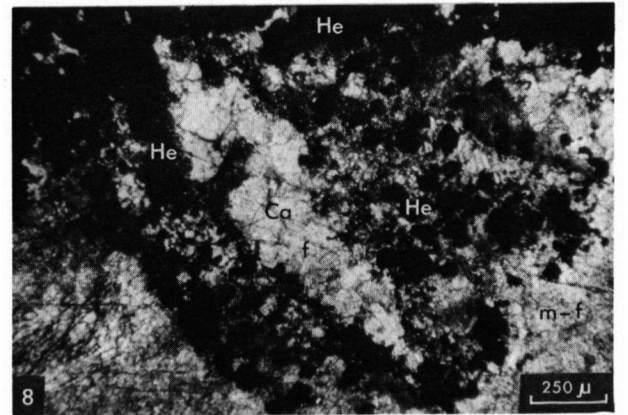
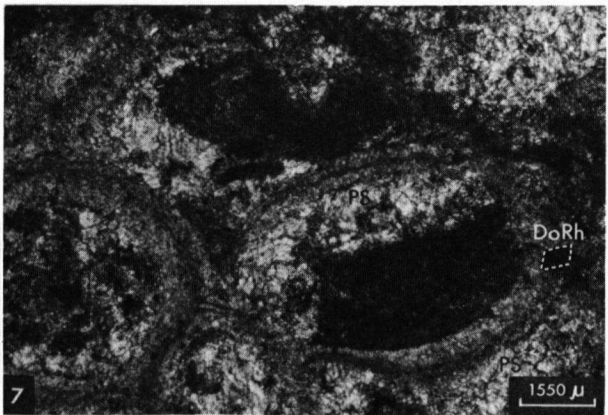
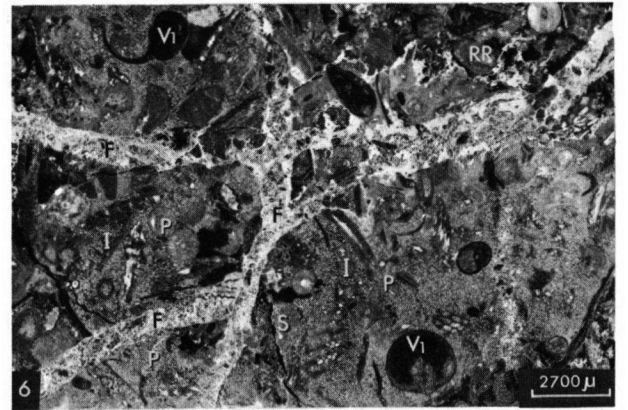
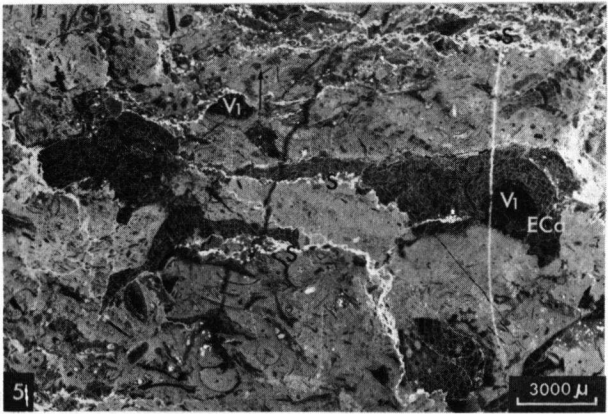
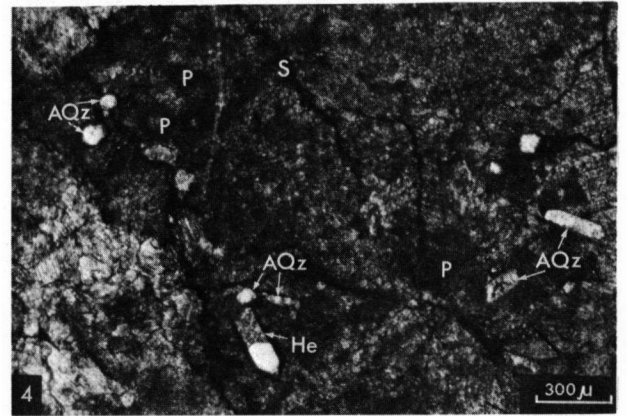
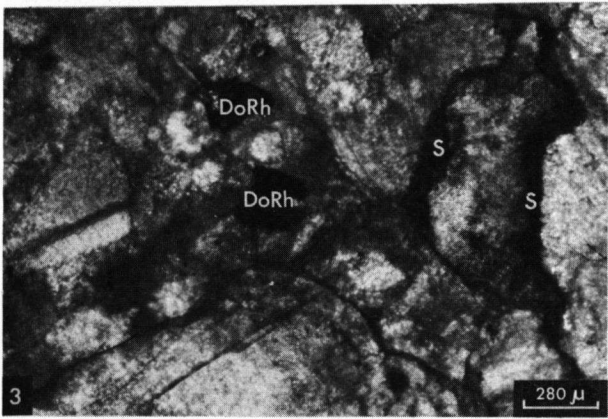
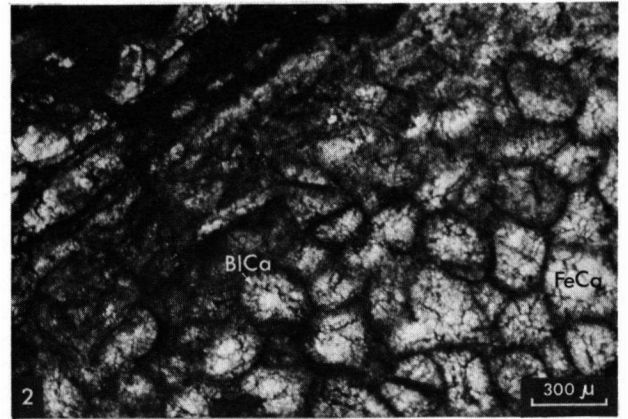
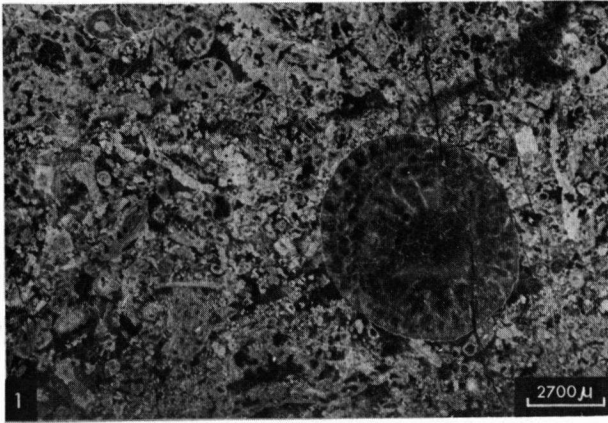


PLATE VII

VII-1. Section 7. Sample 339. Negative photomicrograph. Stained with a mixture of alizarin red S and $K_3Fe(CN)_6$. Facies c. This is a recrystallized wackestone-packstone. Bioclastic debris consists mainly of tabulate corals, crinoids and pelecypods. Interstitial material was originally very finely disintegrated bioclastic material (disintegrated due to scavengers as is proved by the presence of an intersected tube) and mud. Some detrital angular to subangular quartz grains are also present. Recrystallization attacked this material and formed pseudosparite, except in areas protected by large fossil fragments. Around crinoidal fragments syntaxial cement rims are present. Dolomite is present in the form of zoned rhombohedral crystals. These occur preferentially in the pseudosparitic ground mass, in the stylolites and in the cracks. The absence of these dolomitic rhombohedral crystals in the sheltered parts of the ground mass and in the recrystallized fossil fragments is remarkable.

VII-2. Section 20. Sample 13. Stained with a mixture of alizarin red S and $K_3Fe(CN)_6$. Facies d. A biosparudite, containing large fragments of *Ideostroma* sp. (det. Dr. B. H. G. Sleumer, 1969) and some fragments of crinoids (only partly visible). The interstitial material is sparry calcite. The crystals are mainly fine to microcrystalline. Light brown (DoRh) crystals are present, generally possessing a hematite coating. Along certain avenues dedolomitization (DDo) occurs, giving the rhombohedral crystals a corroded and irregular aspect. A few slightly corroded authigenous quartz crystals (AQz) are present. Corrosion indicates that quartz predates dolomite, since dolomite apparently attacks the quartz crystals. The material replacing the dolomite rhombohedral crystals consists of medium to fine (m/f) calcite crystals.

VII-3. Section 5. Sample 377. Negative photomicrograph. Stained with a mixture of alizarin red S and $K_3Fe(CN)_6$. Facies g. In this arenite (packstone-grainstone) we recognize two types of bryozoans, brachiopods, crinoids, gastropods, tentaculites and undeterminable bioclasts. Interstitial material is mainly very finely disintegrated bioclastic material. In a few places we find micrite. The crinoidal fragments show syntaxial cement rims. Rhombohedral dolomite crystals (DoRh), many of which have ferroan dolomitic zones, are scattered throughout the rock. Dedolomitization features are common (arrows). Stylolites and solution stringers (S) divide the thin section into a medium to coarse-grained part (MC) and a fine-grained (F) part.

VII-4. Section 32. Sample 31. Stained with a mixture of alizarin red S and $K_3Fe(CN)_6$. Facies g. (cf. Wolf et al., 1967, Plates XV and XVI). In this grainstone-packstone we distinguish brachiopods, bryozoans, crinoids, ostracods and the activity of blue-green algae. Pellets are scattered throughout the rock. Some angular silt-sized quartz grains are present. The interstitial material is sparite. The irregular corroded aspect of the bioclasts (C) emphasized by the etching acid staining mixture is remarkable. It is the result of boring and encrusting blue-green algae (cf. Wolf, 1967 et al. and pers. comm., Dr. J. J. de Meijer, 1971). The boring tubes are visible in some fragments (arrow).

VII-5. Section 32. Sample 31. Not stained. Facies g. The faunal components in this packstone-grainstone are similar to those of photomicrograph VII-4. The selective encrusting and the resulting grain diminution (Gd) to a silt size is clearly visible. The end of this process is an unrecognizable vaguely ovoid structureless clot, an algal pellet (P). The interstitial material is coarse (ECa); intercrystalline boundaries are straight. Some blade-shaped calcitic crystals (BICa) directly coat the bioclastic fragments. Where these blade-shaped calcite crystals are absent the boundaries between the bioclasts and the (ECa) are very irregular.

VII-6. Section 32. Sample 31. Negative photomicrograph. Stained with a mixture of alizarin red S and $K_3Fe(CN)_6$. The overall picture in photomicrographs VII-4 and VII-5 is that of a coated grain grainstone to packstone. The components do not differ from those already described. The 'umbrella effect' causing a primary void (V₁), which is subsequently filled with very fine material, is clearly visible. Cracks, stylolites and microstylolites (S), often filled with hematitic or ferroan calcite, cross the sample. The entire rock is moderately attacked by recrystallization.

VII-7. Sample 341. Stained with a mixture of alizarin red S and $K_3Fe(CN)_6$. Facies b-c. In this packstone we find compound rugose corals, at least two different types of bryozoans, ostracods and crinoids (not visible). The interstitial material is bioclastic material, which is disintegrated to a silt-size (possibly as a result of grain diminution caused by scavengers). Scattered throughout the interstitial material we find zoned (DoRh) crystals. From the centre of these crystals towards the faces the following sequence is found: (FeDo)-(Fe)Do-(Do)-(Fe). The irregular shape of the faces is due to dedolomitization (DDo). Fractures, stylolites and cracks are present. Some geopetal structures were also observed (not visible in this photomicrograph).

VII-8. Section 26. Sample 76. Stained with a mixture of alizarin red S and $K_3Fe(CN)_6$. Facies b-g. This wackestone contains poorly distinguishable bryozoan fragments, trilobites and crinoids. Pellets and a number of vague ooids are present. The fossil fragments are often silicified. Corroded rhombohedral dolomite crystals occur interstitially. Some have completely disappeared as a result of leaching (DDo). These pores and the corroded rhombohedral dolomite crystals are poikilotopically present in the calcite and in the chert.

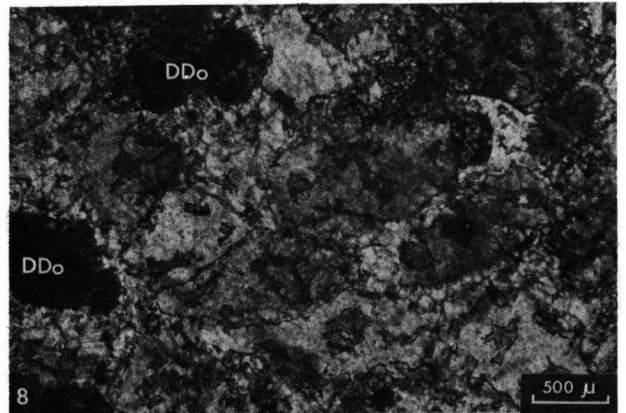
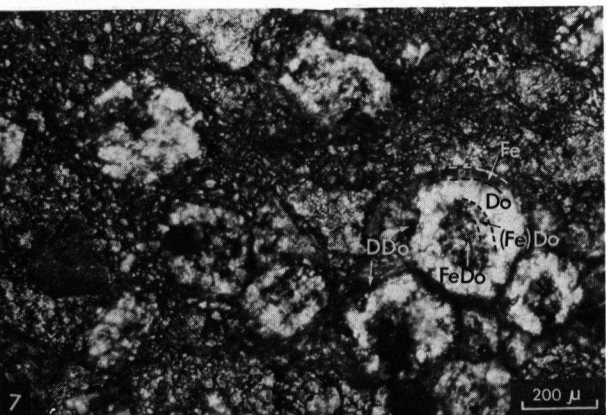
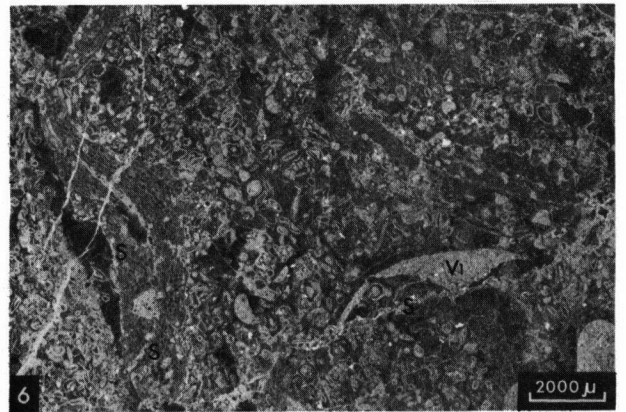
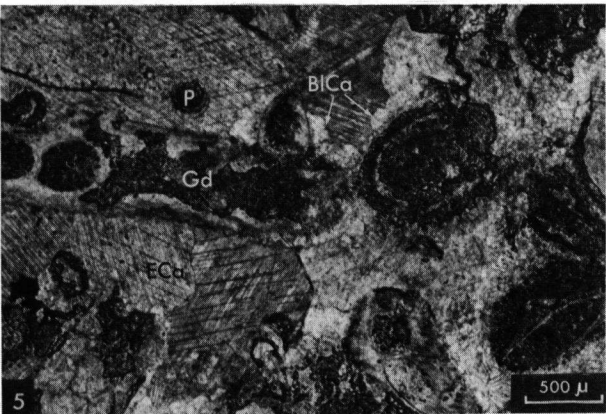
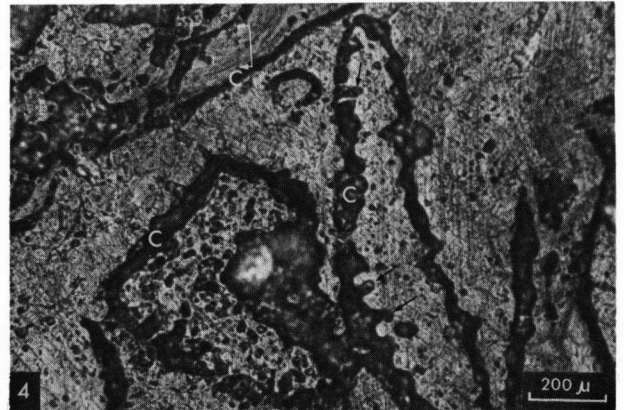
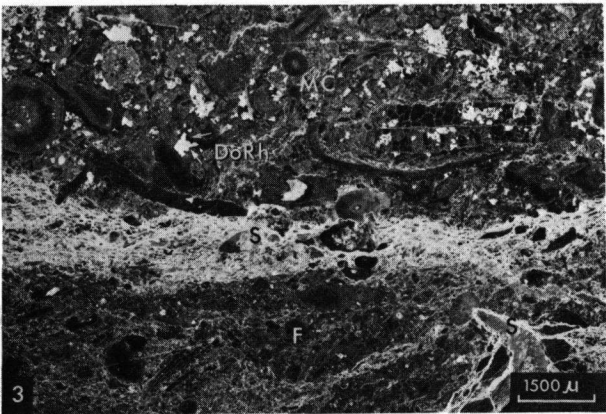
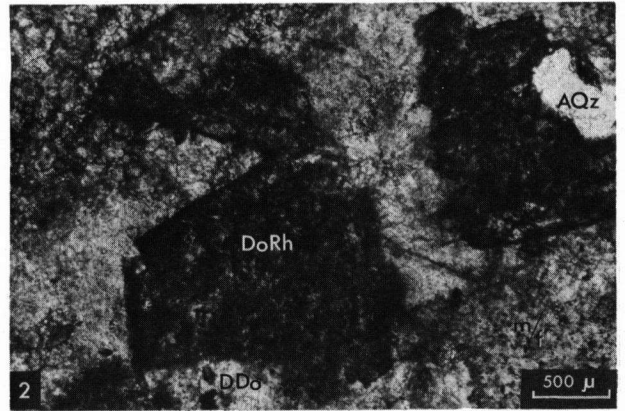
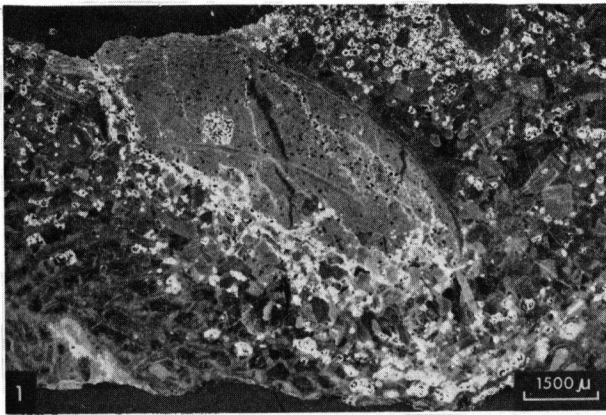


PLATE VIII

VIII-1 & 2. Section 26. Sample 91. Green monochromatic filter. Stained with a mixture of alizarin red S and $K_3Fe(CN)_6$. Negative photomicrographs. Facies b. In these fossiliferous mudstones we chiefly find ostracods and calcispheres. The ground mass is micrite. In a few places pellets are vaguely visible (P). It is presumed that the ground mass is predominantly pelletoid, but these structures are obscured. Primary voids are present in the inter-fossil spaces (V_1) and along fractures. In addition some sparite-filled vugs (V_2) are present, sometimes partly filled with a sedimentary floor (Bird's eye limestone). Bubble-like authigenic hematite, clustered in pellets, is present in the basal sediments (He). The remaining space in these vugs is filled with sparry calcite (ECa). At least three generations of fractures (F) postdate the void filling material.

VIII-3. Section 27. Sample 203. Not stained. Negative photomicrograph. Facies b. A fossiliferous micrite with a few transported larger fragments of corals as well as (not visible) ostracods, gastropods and calcispheres. Pellets are common. Tiny vugs, filled with rimming blade-shaped calcite crystals (BCa) and with (ECa) in the centre, are common. Some have basal sediments. The blade-shaped calcite crystals cause the light halo that coats the walls of the void.

VIII-4. Section 31. Sample 225. Negative photomicrograph. Stained with a mixture of alizarin red S and $K_3Fe(CN)_6$. Facies b. In this fossiliferous mudstone we find a large quantity of pellets (P), some ostracods and especially calcispheres. Microscopic vugs (?) are distributed over the sediment in a patchy way. They are rimmed with (BCa) and filled with blocky cement (ECa). Some of these vugs are partly filled with basal sediments consisting of silt-sized bioclastic debris and larger grains.

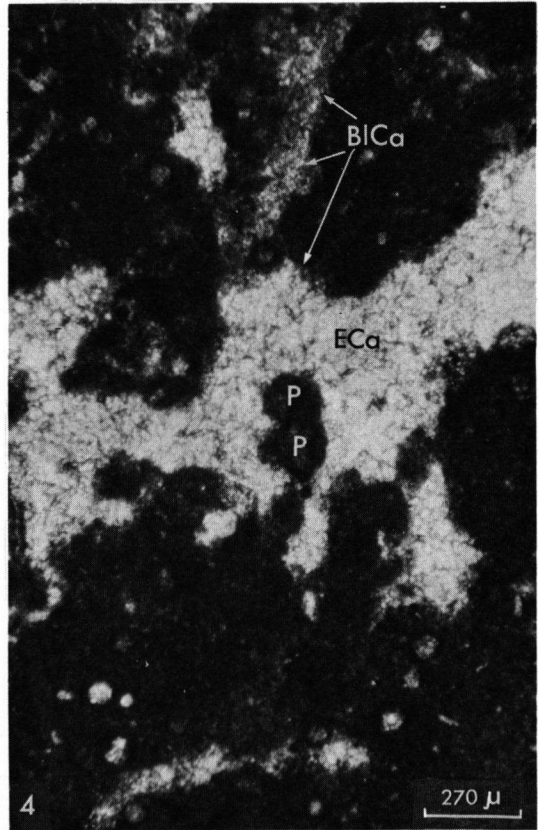
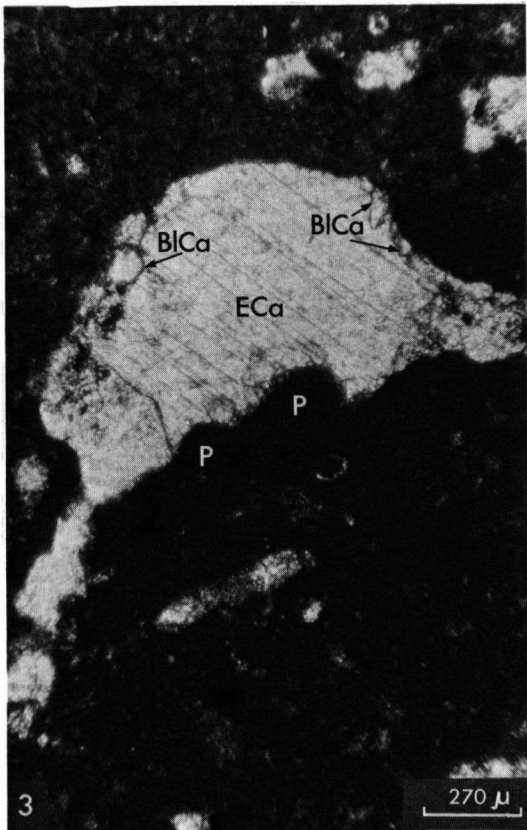
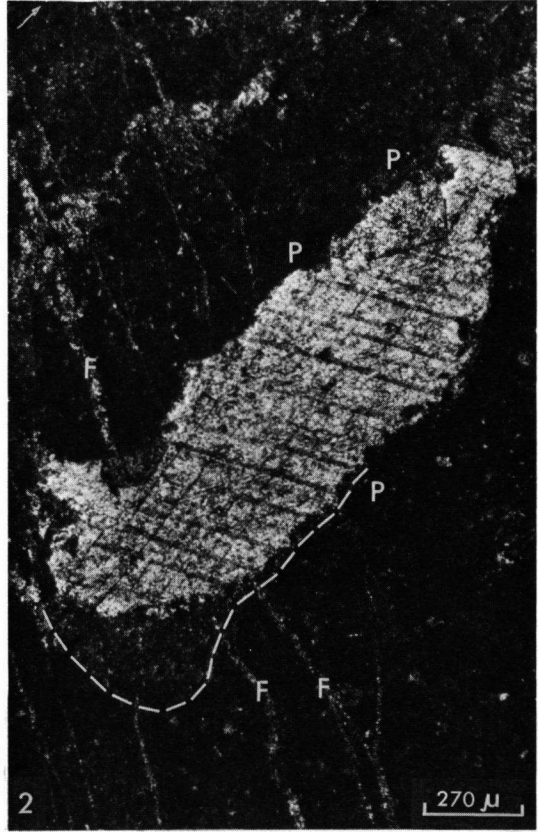
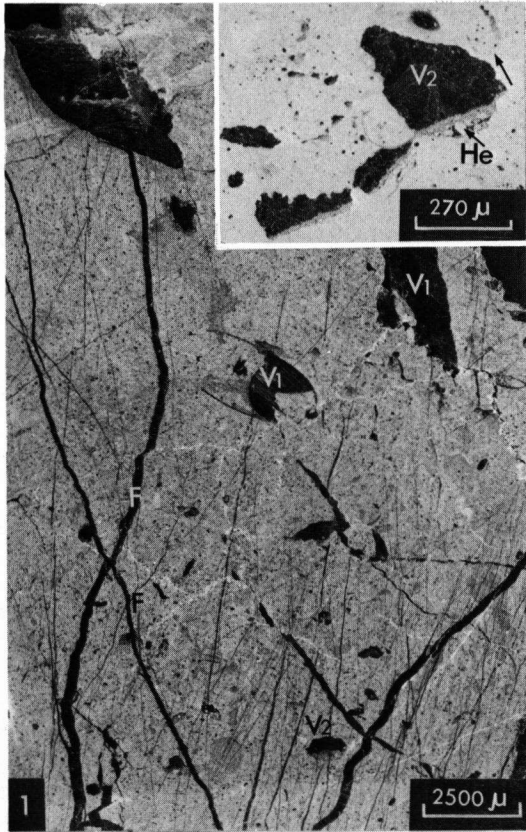


PLATE IX

IX-1. Section 33. Thirty-five metres from base (cf. Pl. IV-3). Facies b. A regular, slightly wavy, medium-bedded sequence. The contacts between the layers are somewhat stylolitic which results in a pseudo-nodular appearance. Colour is medium grey. The faunal components are zaphrentoid rugose corals, branching tabulate corals and ostracods.

IX-2. Section 15. Forty metres from base (cf. Pl. IV-4). Facies c-e. A packstone, composed of debris from compound (C) rugose corals, platy (Pl) and ramose (Ra) tabulate corals, stromatoporoids (St), bryozoans and a few crinoidal fragments. Bedding is irregular and often indistinguishable. The general depositional direction is mainly indicated by means of stylolites.

IX-3. Section 29. Fifty to fifty-four metres from the base. Facies g. A cross-bedded, partly decalcified, limestone layer, with vugs in a siliciclastic interval. Pronounced sedimentary structures are rendered visible by weathering.

IX-4. Section 4. Sample 441. Negative photomicrograph. Stained with alizarin red S and $K_3Fe(CN)_6$. Facies b. In this wackestone-like packstone we distinguish brachiopods, pelecypods, calcispheres, ostracods and trilobites. The interstitial material is very finely grained bioclastic matter (diminished in size). In a few places it is micrite. Neomorphously formed pseudospurite is present in small patches. Primary voids formed by the 'umbrella effect' are often filled with equant calcite (ECa). Primary depositional structures are vaguely recognizable. Sometimes stylolites (S) are present, filled with ferruginous material and accentuating these primary depositional structures. It is clearly visible that the larger bioclastic fragments have been attacked, presumably by physicochemical processes, and are therefore diminished in size. Sometimes only ghosts (G) are present.

IX-5. Section 26. Sample 92. Negative photomicrograph. Stained with a mixture of alizarin red S and $K_3Fe(CN)_6$. Facies b. Many ooids are present in this calcarenite. The recognizable bioclastic fragments are crinoids, bryozoans and ostracods. They sometimes have syntaxial grain growth rims. Pellets are also present (P), sometimes concentrated in patches. Many detrital quartz grains and some idiomorphic authigenic quartz grains are present. Microstylolites (S) of the pressure solution type are present parallel to the primary depositional direction and accentuate this, as do fining upwards structures. The sizes and the irregular shapes of the ooids suggest that we are dealing with a pisolite (cf. Pl. IX-3). Signs of algal coating are often clearly visible. The outer walls of the algal coated ooids have a worn appearance which is partly produced by borings (cf. Pl. IX-6). The bored openings are filled with hematitic material (He).

IX-6. Section 26. Sample 92. Negative photomicrograph. Stained with a mixture of alizarin red S and $K_3Fe(CN)_6$ (cf. Pl. IX-5). Facies b. From this figure it is evident that the pisolite contains concentrically coated grains with a crenulated appearance. The outermost layer is partly attacked by boring algae (A). This bored surface is filled with hematitic (He) material. The same holds for the crinoid fragment. Hematitic pellets are scattered throughout the sample. The interstitial material is cement formed by fine equant calcite crystals. The intercrystalline boundaries are often serrated and irregular.

IX-7. Section 4. Sample 442-A. Negative photomicrograph. Stained with a mixture of alizarin red S and $K_3Fe(CN)_6$. Facies b. In this sandstone we mainly find very fine quartz sand with some glauconite grains, hematite and calcite (cement). Some rhombohedral dolomite crystals are present. The quartz sand grains are subrounded to angular. They are often coated with a hematite crust. In the burrow tube the quantity of dolomite (Do) and of hematite is significantly larger than in the host rock which is therefore lighter in colour. Some quartz grains, especially in the burrow tube, show authigenic enlargements. Depositional laminations (L) are rendered visible by a regular alternation of layers with a different orientation of the longest axis of the grains. The contacts between many grains are pointlike. Cement is calcitic. The primary depositional structure is slightly disturbed. Dragging caused by burrowing animals is visible (D).

IX-8. Section 27. Sample 205. Negative photomicrograph. Stained with a mixture of alizarin red S and $K_3Fe(CN)_6$. Facies c. Packstone, partly boundstone. Here we find colonial tabulate corals, compound rugose corals (not visible), bryozoans, crinoids and many unrecognizable bioclastic fragments. Recrystallization has moderately attacked the rock. Grain contacts are microstylolitic. These microstylolites are often filled with hematitic material and sometimes with zoned rhombohedral dolomite crystals. Grains are somewhat flattened. Interstitial material is very finely grained bioclastic material.

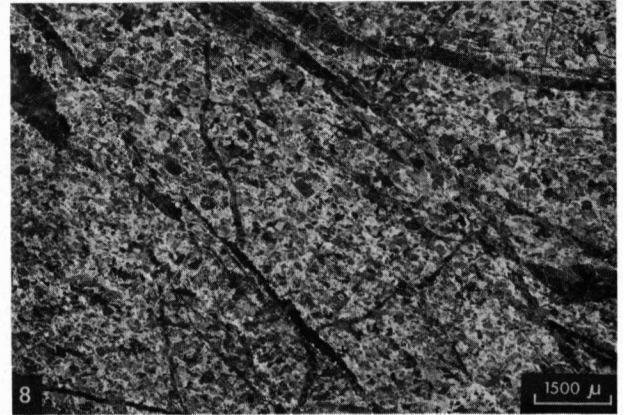
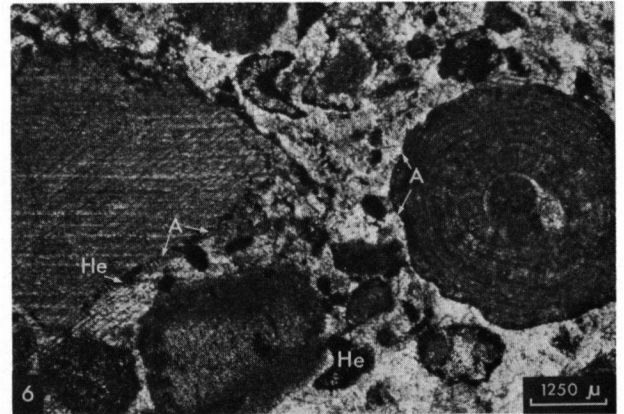
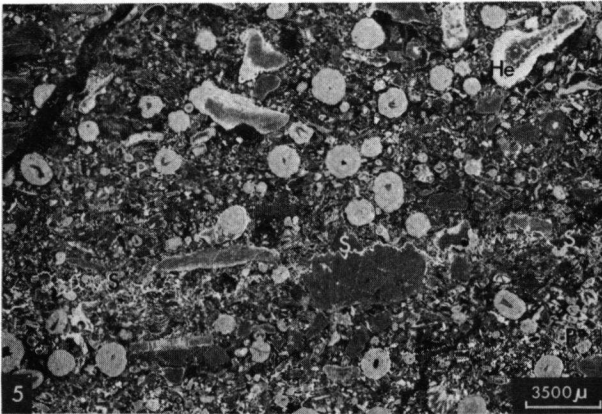
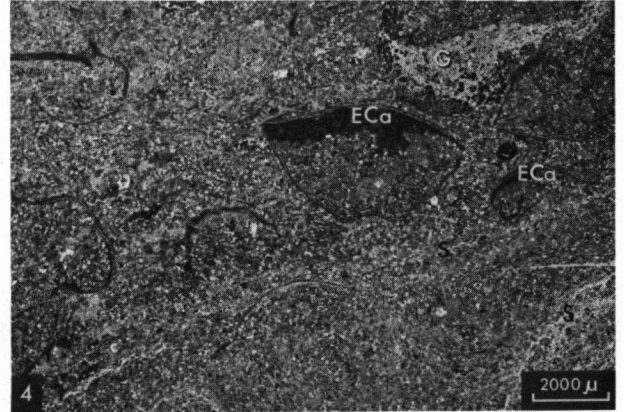
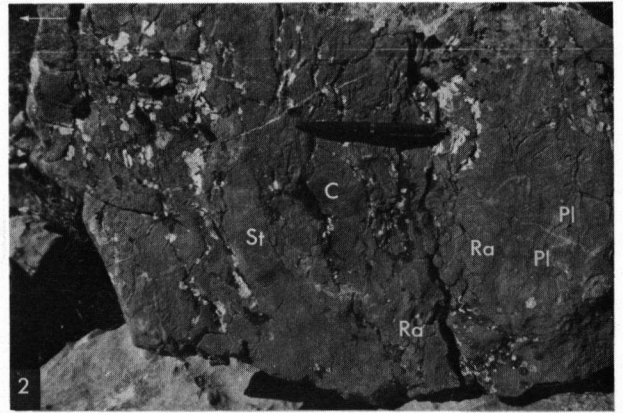


PLATE X

X-1. Section 28. Sample 50. Negative photomicrograph. Stained with a mixture of alizarin red S and $K_3Fe(CN)_6$. Facies c. In this typical boundstone we find branching tabulate corals, stromatoporoids, compound rugose corals and some scattered crinoidal particles. The corals show close interrelation. The contacts are stylolitic (S). The stylolites (of the pressure solution type) are filled with hematitic material. Strong solution phenomena were observed. The rock is moderately attacked by recrystallization.

X-2. Section 29. Sample 174. Negative photomicrograph. Stained with a mixture of alizarin red S and $K_3Fe(CN)_6$. Facies g. In this sandy limestone we find crinoidal debris and fragments of brachiopods. A considerable amount of very well rounded, moderately sorted quartz grains is present. Recrystallized patches are scattered throughout the sample. A depositional structure is vaguely visible (arrow indicates top). In a few places syntaxial cement rims occur around the crinoidal fragments. The contacts between the grains are often stylolitic. Pressure solution can be seen.

X-3. Section 5. Sample 381. Stained with a mixture of alizarin red S and $K_3Fe(CN)_6$. Facies c. In this sample it is clear that dedolomitization (DDo) processes attacked the dolomite rhombohedral crystal (DoRh) in two places because it has a worn aspect as a result of the partial replacement by (Fe)Ca.

X-4. Section 5. Sample 380. Stained with a mixture of alizarin red S and $K_3Fe(CN)_6$. Negative photomicrograph. Facies g. In this silty packstone we find at least two types of bryozoans, ostracods and brachiopods. A depositional structure is vaguely visible (arrow). Geopetal structures are common as well as trapping of very finely grained detrital material. Micro slumps were seen. Hematitic material occurs in abundance at certain levels (He).

X-5. General view of the biohermal zone in the vicinity of section 22. The massive mound-like structures (B) are partly covered by a nodular 'envelope' (E). It is more likely for the latter to be weathered than for the massive moundlike structures. A joint pattern stresses the general biohermal shape.

X-6. Section 22. Photograph from east to west. Member D of the Portilla Limestone Formation. On the right hand side of this photograph the nodular layers (N) that are interbedded in the biohermal sequence are clearly visible. Bedding is slightly wavy, presumably due to local differences in load. Arrow indicates top.

X-7. Section 22. Photograph from east to west. The scree sediments (S) abut against the massive biohermal sequence (B). In this latter some vague erosional surfaces (E) are visible. The scree sediments are locally composed of a regular alternation of layers containing fossils in growth position and fossils that have been somewhat transported (cf. Fig. 8).

X-8. Section 10. Sample 10. Stained with a mixture of alizarin red S and $K_3Fe(CN)_6$. Facies b. Bioclastic medium calcarenite containing fragments of bryozoans, brachiopods and ostracods. The sorting and roundness of the fragments is good. The interstitial material (not visible) is composed of equant calcite crystals with rather straight intercrystalline boundaries. Some of the grains have a dark (hematitic; He) coating. The equant calcite cement was precipitated after the coating with hematite occurred. Dolomite is present in the form of rhombohedral crystals (DoRh) and as irregular anhedral patches (Do). The (DoRh) can be worn and slightly attached by leaching and by other processes. They occur in the intergranular space. The anhedral patchy dolomite occurs preferentially in the bioclastic grains.

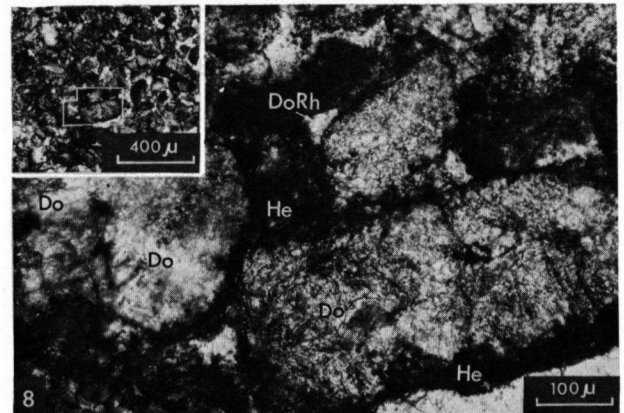
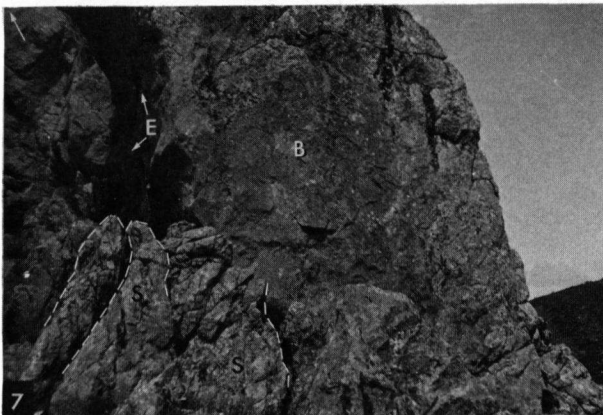
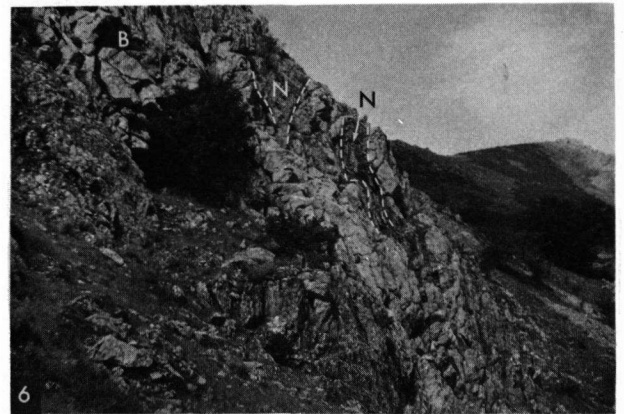
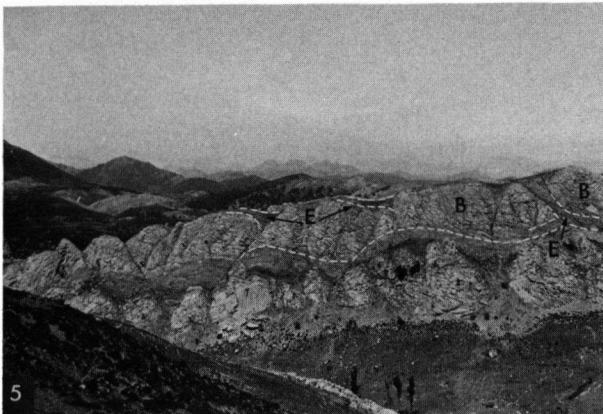
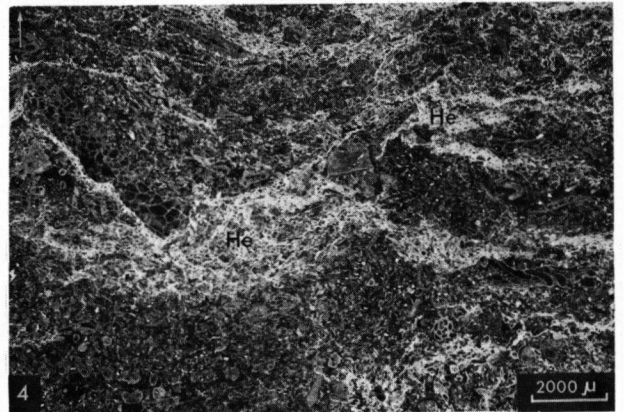
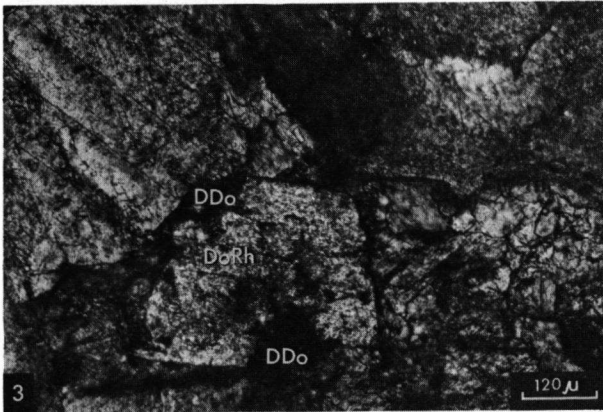
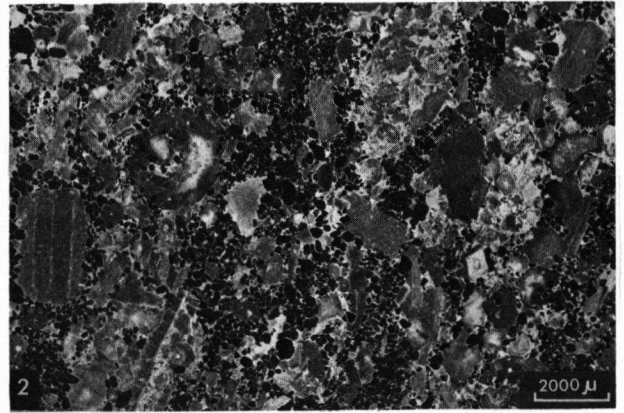
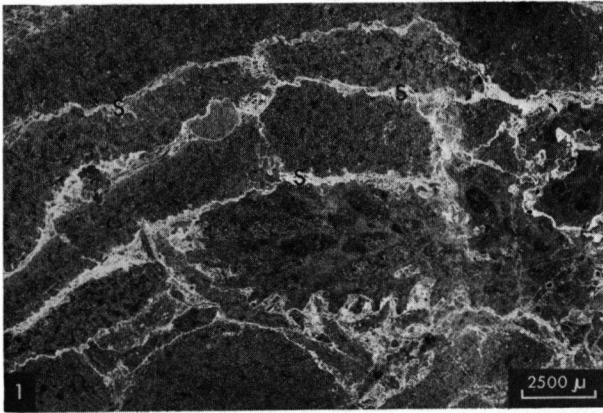


PLATE XI

XI-1. Section 12. Sample 3. Stained with a mixture of alizarin red S and $K_3Fe(CN)_6$. Facies b-c. In this medium crystalline (fc) calcite mosaic (pseudosparite), consisting of crystals of varying sizes, the larger ones of which are bioturbation, too, were observed. The interstitial material is a neomorphic medium crystalline (mc) to fine crystalline (fc) calcite mosaic (pseudosparite), consisting of crystals of varying sizes the larger ones of which are sometimes rimmed by very fine crystals (vfc). The bioclastic fragments often, show grain diminution phenomena. Dolomite crystals, presumably ghosts of rhombohedral crystals (DoRh) occur in the mosaic of calcite crystals. They have a strongly corroded surface with (fc) calcite embayments presumably produced by dedolomitization.

XI-2. Section 14. Sample 168. Stained with a mixture of alizarin red S and $K_3Fe(CN)_6$. Facies b. In this packstone much fuzzy sponge-like ferruginous material (He) occurs between the bioclasts. Characteristic of this sample is the occurrence of secondary pores produced by selective leaching and dissolving of (DoRh) crystals. Ghosts like outlines of these crystals are still present and the rhombohedral shape of the pores prove the earlier presence of (DoRh).

XI-3. Section 14. Sample 169. Stained with a mixture of alizarin red S and $K_3Fe(CN)_6$ (cf. Pl. XI-3). Facies b. Here the interstitial material is not sponge-like ferruginous material, but fine crystalline calcite or fine crystalline patchy dolomite (fc). The pores are filled with (DoRh). Due to the acid liquid used for staining, the level of the dolomite crystals is now somewhat lower. A dark rim (Ri) is visible around the pores in the host rock. This is ferruginous material, presumably expelled by the (DoRh) crystals during secondary growth. Dedolomitization phenomena are visible, beginning both in the centre of the crystals and around the faces.

XI-4. Section 16. Sample 9. Crossed nicols. Stained with a mixture of alizarin red S and $K_3Fe(CN)_6$. Facies b. In this biopelsparite bioclastic fragments are generally unrecognizable. Interstitial material is a very fine, a fine or a medium coarse (vf, f, m) mosaic of (Fe)Ca to (Fe)Do. The occurrence of subhedral dolomite crystal patches and of a few euhedral dolomite crystals, pseudomorphous after (authigenic?) quartz, is remarkable. Some relic fragments of the quartz are still visible. There are extreme differences in grain sizes. The mosaic calcite or dolomite crystals are rimmed by very fine calcite and/or dolomite crystals. The intercrystalline boundaries are generally fairly straight.

XI-5. Section 18. Sample 9. Stained with a mixture of alizarin red S and $K_3Fe(CN)_6$. Facies b. This micrite is neomorphically changed into microsparite which is crossed by many cracks and stylolites. In the ground mass much ferruginous material is present. Some muscovite flakes were observed. The ground mass is mainly composed of calcite (dark patches). Dolomite (Do) patches (light patches) also occur and have fairly straight boundaries. The (Do) is subhedral to euhedral and crystal sizes are fine to very fine (f, vf). The (Ca) is euhedral and crystal sizes are medium (m). The euhedral to subhedral (Do) crystals are of replacement origin as is proved by relics of calcite and by the dusty appearance. In the centres of the light patches (Do) crystals are dustier (D) than around the outlines.

XI-6. Section 16. Sample 1. Crossed nicols. Stained with a mixture of alizarin red S and $K_3Fe(CN)_6$. Facies b. In this packstone we find fragments of bryozoans, crinoids and brachiopods. Burrow tubes (B) occur. They are often filled with a fairly important quantity of ferruginous material and with argillaceous material. Many bioclastic grains, diminished in size, occur preferentially in the tubes. The bioclastic material and the ground mass is often (Fe)Ca to (FeCa). Small bioclastic fragments have extremely irregular surfaces, caused by grain diminution (GD).

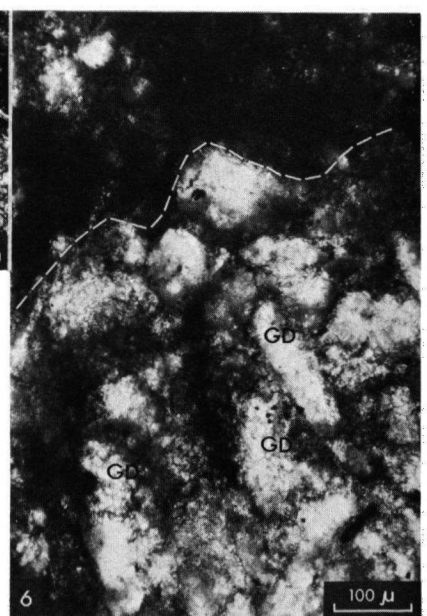
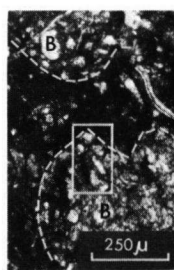
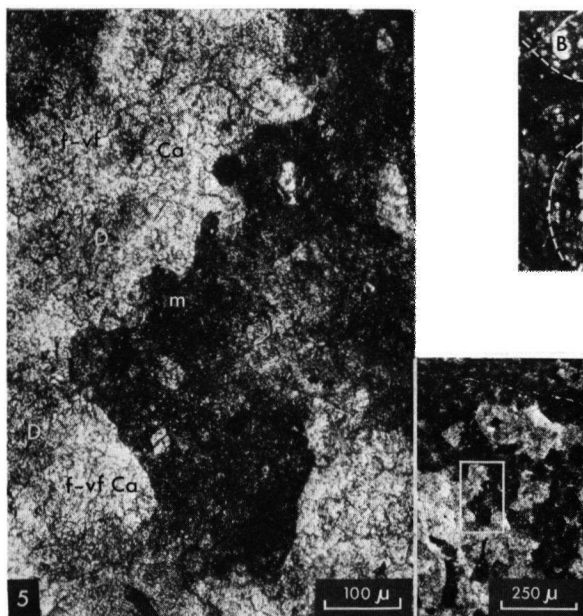
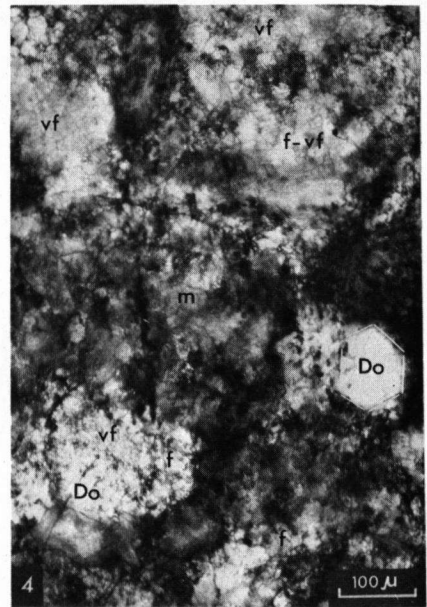
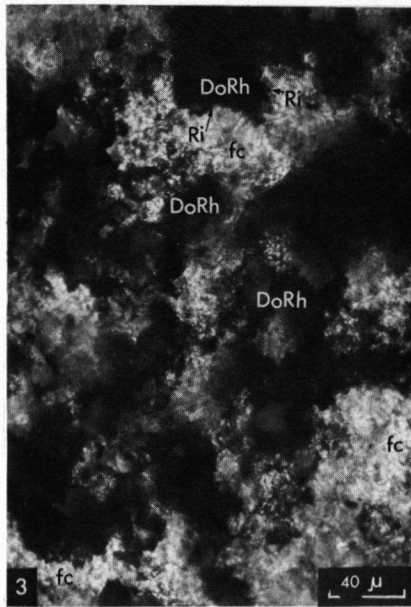
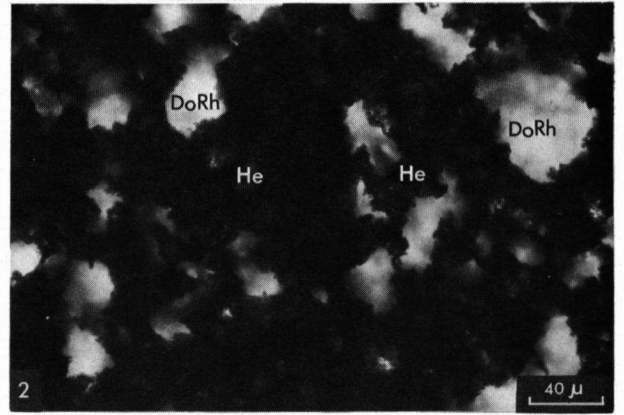
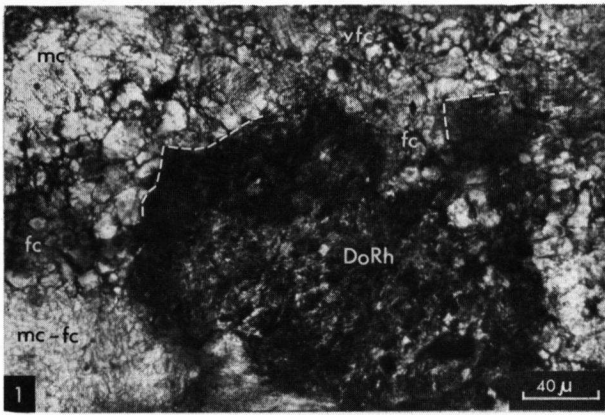


PLATE XII

XII-1. Section 20. Sample 17. Stained with a mixture of alizarin red S and $K_3Fe(CN)_6$. Facies b. In this biomicrite large bioclasts, like zaphrentoid rugose corals, occur (not visible) which are filled with micrite. Aggrading neomorphic processes of micrite into simple microsparite crystals have already begun. Chert (Ch) grows in irregularly distributed locations throughout the sample. The outlines of the micrite and/or microsparite crystals are vaguely visible as impurities in the chert (Z). These zones of impurities were possibly formed during the postulated primary aragonite mud to micrite/microsparite inversion process. The scattered rhombohedral dolomite crystals were formed during silification since impurities, expelled by the growing (DoRh) crystals, are present in the chert around the (DoRh) crystals. Large crystals occur in or near the borders of larger chert patches. Small (DoRh) crystals are scattered at random throughout the rock. Sometimes only rhombohedral pores (RhP) occur as a result of leaching processes. A number of fractures, filled with coarse (ECa), cross the sample and postdate all above-mentioned processes.

XII-2. Section 28. Sample 62. Negative photomicrograph. Stained with a mixture of alizarin red S and $K_3Fe(CN)_6$. Facies b. In this pelletal bioclastic grainstone ostracods and crinoids are recognizable. The pellets are ovoid to circular. Some have dark micritic zones. In a few cases boring was observed. This might indicate the activity of algae. The interstitial material is sparite. There is a tendency towards bladed calcite crystals immediately around the pellets and (ECa) calcite crystals in the centres of the interstitial voids. Burrowing animals produced a slightly disturbed sediment (B). The distribution of the pellets slightly accentuates a depositional lamination, since there are fine pellets (FP) and medium pellets (MP). In some locations dolomitization (DoRh) and a few dedolomitization features are visible.

XII-3. Section 29. Sample 168. Facies b. This is a wackestone with various bioclasts. Part of an ostracod is visible. Inside and around this fossil vague clot-like ovoid grains (pellets, P) are recognizable. The ostracod is changed into medium (ECa) crystals (pseudosparite) by neomorphic aggrading processes. Not all the fossil fragments are changed in this sense. The interstitial material between the pellets consists of fine calcite crystals with fairly straight intercrystalline boundaries.

XII-4. Section 5. Sample 389. Stained with a mixture of alizarin red S and $K_3Fe(CN)_6$. Facies b. In this packstone-grainstone we find fragments of compound rugose corals, pelecypods, bryozoans, crinoids and ostracods. Some undeterminable clots [presumably pellets (P)] were also observed. In a few places there are indications of burrowing activity. The interstitial material is extremely interesting. Some bioclasts are rimmed with fibrous calcite crystals. Larger interstitial patches are occupied by blocky (Fe)Ca cement crystals showing serrated intercrystalline boundaries. The sizes of the crystals vary considerably between medium and fine (mc, fc). Towards the boundaries of the crystals and the ground mass there is a tendency towards smaller crystals. A number of rhombohedral dolomite crystals, partly replaced by calcite (dedolomite), are present in these larger interstitial patches. They occur mainly near the boundaries of the patches. Some fossil fragments (here presumably calcispheres) are largely and selectively replaced by hematite (He). In addition, patchy anhedral dolomite crystals are present scattered throughout the sample.

XII-5. Section 29. Sample 176. Negative photomicrograph. Stained with a mixture of alizarin red S and $K_3Fe(CN)_6$. Facies b. In this wackestone-packstone we mainly find ostracods, bryozoans (two types), fragments of trilobites, crinoids and gastropods. Some fragments of uncertain origin, most probably rounded intraclasts (I), are present. Cracks postdate all features. Microstylolites (S) often surround the grains. Some bioclasts are coated with hematite (He). Hematite patches are present, scattered throughout the ostracod fragments. The interstitial material is microsparite (small equant crystals), presumably produced by neomorphic aggrading processes. Many of the bioclastic fragments, especially the ostracods, have been neomorphically changed into medium calcite crystals.

XII-6. Section 11. Sample 12-1. Stained with a mixture of alizarin red S and $K_3Fe(CN)_6$. Facies c. This is a packstone with, in a few places, the aspect of a boundstone (not visible). Many different types of corals, crinoids and brachiopods are present. In the interstitial space hematitic material, very fine granular calcite (FeCa) crystals, and strongly corroded (zoned) (DoRh) are present. The centres of these (DoRh) are generally calcitic (dedolomite); the surface, however, is still (Fe)Do to (Do). These (DoRh) are often present in the immediate vicinity of very fine (vf) to fine (f) irregular crystalline (F)Ca cement. The calcite crystals and grains are strongly interlocked, but they show an extreme difference in size. A number of fractures (F) filled with (Ca) cross the sample.

XII-7. Section 22. Sample 612. Negative photomicrograph. Stained with a mixture of alizarin red S and $K_3Fe(CN)_6$. Facies type c. Packstone-boundstone. *Thamnopora* sp., *Coenites* sp., ostracods, crinoids, calcispheres and recognizable bioclastic fragments. Some undetermined clasts, possibly intraclasts (I), are present. The interstitial material is very finely grained detrital to micritic material. In a few places initial chertification (Ch) is visible. Very fine crystalline silicious material is preferentially clustered in coral theca, giving the appearance of chert patches. Between the bioclasts solution stringers (S) and stylolites occur. In these stylolites hematitic (He) and shaly material is present.

XII-8. Section 8. Sample 334. Not stained. Facies c. In this sample we find micrite which is neomorphically changed into microsparite (MS) in the inter-particle space. In this microsparite (ms) light brown rhombohedral dolomite crystals are present. The microsparite crystals have sometimes replaced (R) parts of the (DoRh) (dedolomitization). The contacts are serrated. Fractures (F) cross the microsparite and the rhombohedral dolomite crystals, postdating the above-mentioned phenomena.

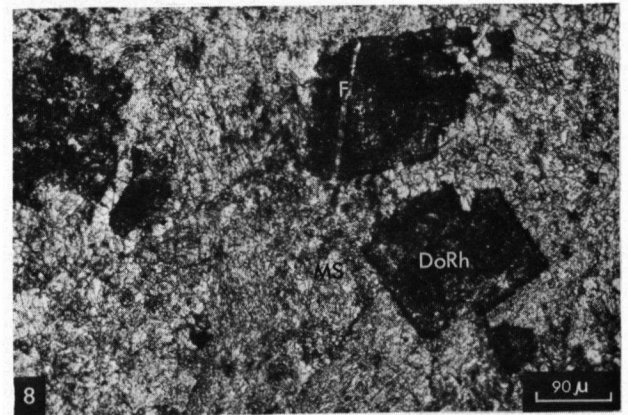
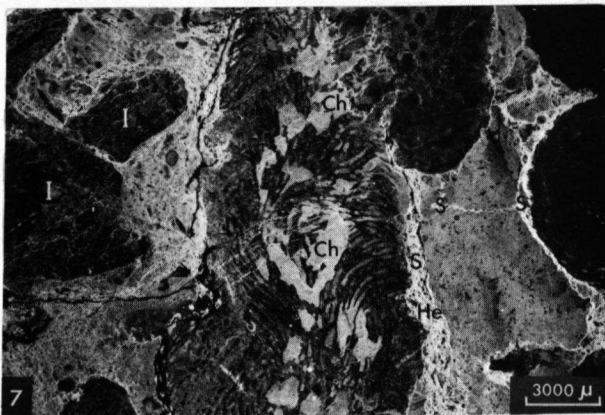
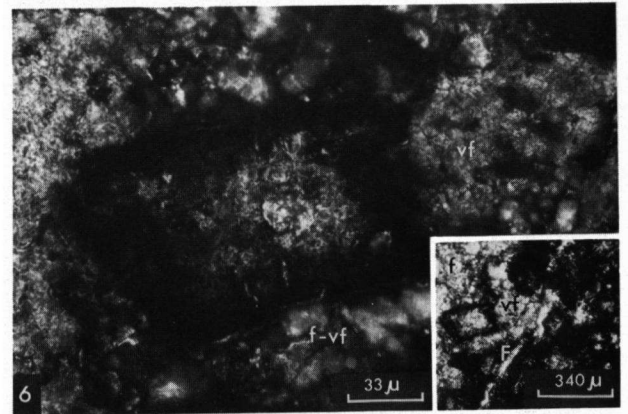
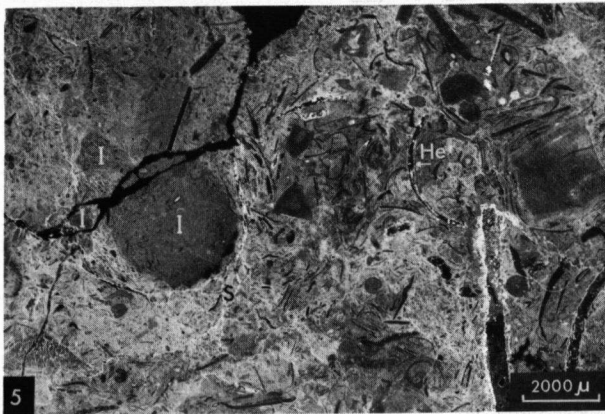
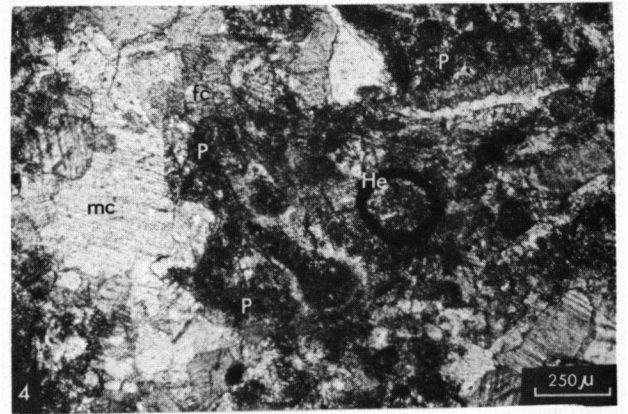
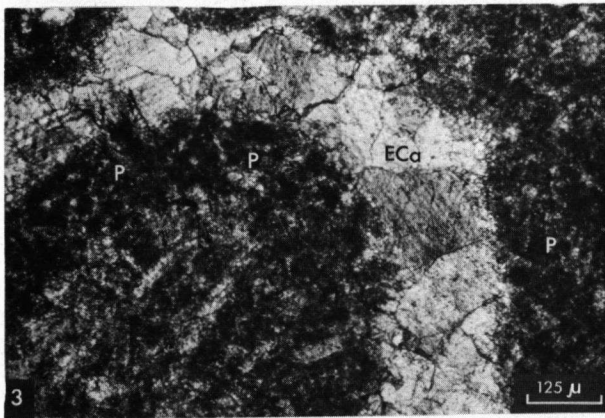
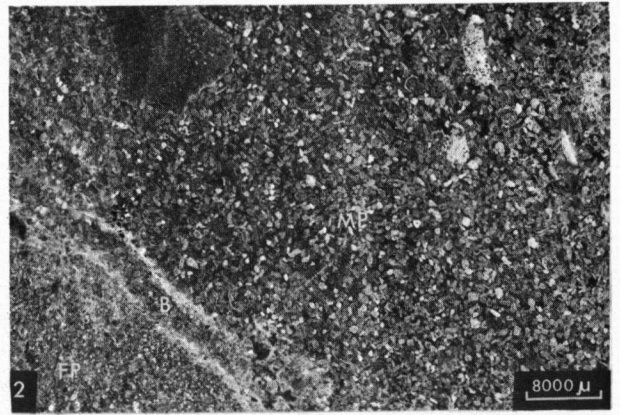
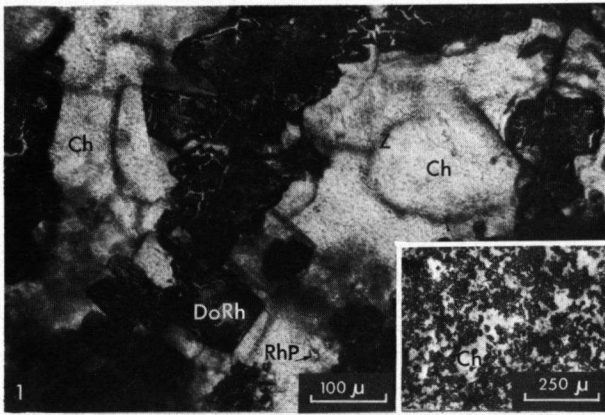


PLATE XIII

XIII-1. Section 3. Sample 401. Stained with a mixture of alizarin red S and $K_3Fe(CN)_6$. Facies c. In this packstone to boundstone we mainly find branching tabulate corals, bryozoans, gastropods and crinoids (only partly visible). Some undetermined bioclastic grains and some pellets are present. The interstitial material consists of very finely grained (Fe)Ca bioclastic material and some micrite. Stylolites and fractures are present in great quantities. The corals are often silicified. Rhombohedral dolomite crystals are present in the theca of corals and have straight boundaries. They are not attacked by chert. The cracks (at least two generations) postdate silicification; (FeCa)/(FeDo) containing liquid was presumably introduced along the avenues created by the cracks, since they are filled with (Fe)Ca and (Fe)Do material.

XIII-2 & 3. Section 22. Sample 619. Green monochromatic filter. Facies c. This is a packstone-boundstone. The interstitial material is (Fe)Ca to (Ca) cement in medium crystals with fairly straight intercrystalline boundaries. In this ground mass dark brown (DoRh) are present. They possess coatings of hematitic material and are uniformly coated with a rim of clear fine (Ca) crystals, exactly following the outer surface of the coated (DoRh). The outer side of this rim is a dark halo (H) presumably produced by expulsion of undigested impurities out of the (DoRh) crystals. After 12.1 % shrinkage of the replacing (DoRh) a clear white rim of calcite could be precipitated out of the fluid, containing calcite.

XIII-4. Section 5. Sample 388. Stained with a mixture of alizarin red S and $K_3Fe(CN)_6$. Facies c. In this packstone we find many fossil fragments, of which an ostracod (O) is recognizable. It is present in a ground mass of very fine crystalline calcite and some dolomite. Some (DoRh) are present in this ground mass. They can be pure (Do), (Fe)Do and (FeDo). Patchy anhedral (Do) is also present. In the ostracod we find rimming with (BiCa) to fibrous calcite crystals while the centre is filled with (FeCa) equant crystals and some (Do) patches. Definite hematite (He) grains occur at random. In a few cases (not visible in this photomicrograph) the (FeCa) equant crystals in the centre of the voids are reduced in size by grain diminishing processes.

XIII-5. Section 32. Sample 36. Negative photomicrograph. Stained with a mixture of alizarin red S and $K_3Fe(CN)_6$. Facies f. In this moderately recrystallized calcarenite crinoidal and brachiopodal fragments are recognized. The contacts between the grains are generally stylolitic (S) or microstylolitic and dissolution occurs. In stylolites subrounded quartz grains are present. The original interstitial material is unknown. It is now (Fe)Ca. Some cracks postdate the deposition of the bioclasts, and are also filled with (Fe)Ca.

XIII-6. Section 28. Sample 40. Stained with a mixture of alizarin red S and $K_3Fe(CN)_6$. It can easily be seen in this photomicrograph that the syntaxial rim cement around the crinoidal fragment shows a differentiation into a purely calcitic part (Ca) and a (Fe)Ca part. The part in the rimming cement that contains iron is not uniform in composition, but shows alternation of lighter and darker stained zones. From similar observations, Evamy & Sherman (1964) concluded that the origin of the syntaxial rim cement was most probably early precipitation of cement in open voids and not, as advocated by Bathurst (1958), replacement.

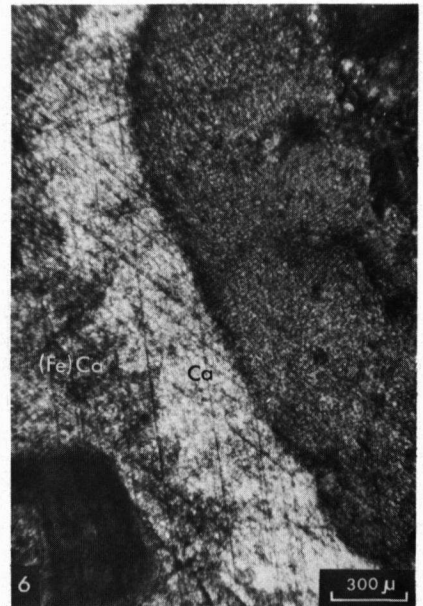
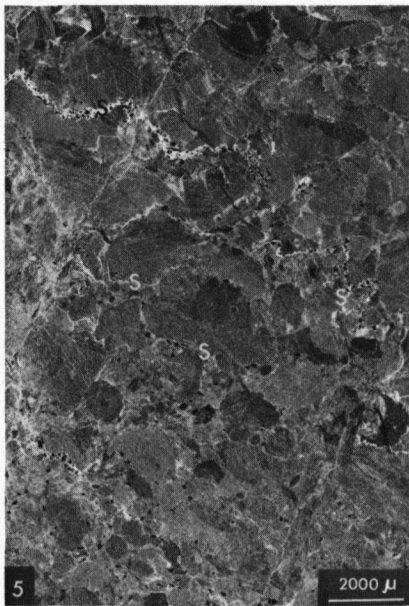
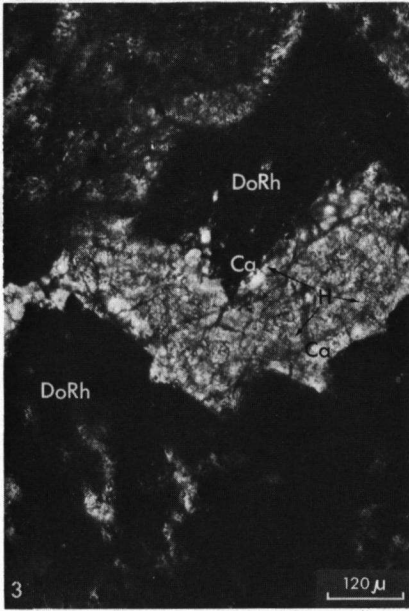
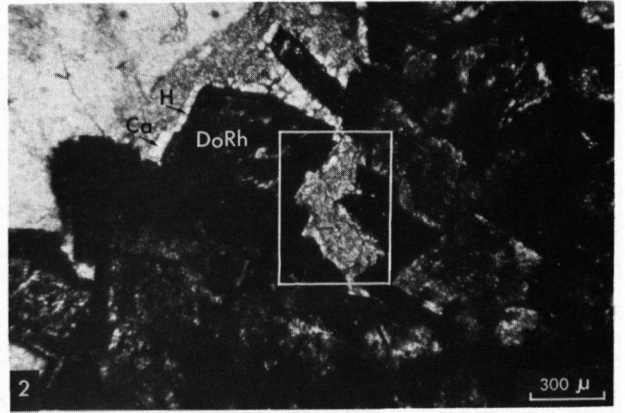
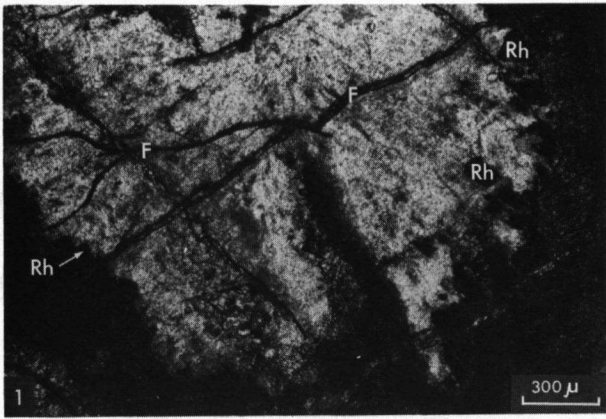


PLATE XIV

XIV-1. General view of area between sections 28 and 29 (cf. Encl. III). Dip of the undisturbed layers 35° towards the north (350°). Left is NW, right is SE. Letters represent facies recognizable in the field (cf. Figs. 11, 12). Member B is divided by a locally important discordance plane (cf. Fig. 11). In the upper part of Member B an important change in facies is visible. From the NW towards the SE, sediments are successively developed as thick-bedded, massive, light grey (N 7) limestone (facies c) with abundant amounts of massive and platy corals, and in a well bedded medium layered dark gray (N 4) limestone (facies b). The bedding contacts are often stylolitic. Shaly material is present in the stylolites. A similar facies change occurs also in the lower part of Member B, where c facies abruptly changes into b and g facies.

XIV-2. The change in facies from the massive, light coloured facies c sediments into the thinner layered, darker facies b sediments.

XIV-3. Gravitational features (slumping), present in the sediments below the discussed facies changes. The layers above the slumped level are undisturbed. The slumping layers dip 31° towards the NE (69°), while the general dip of the undisturbed beds is 35° towards the north (350°) as is visible in Pl. XIV-1. No traces were found of faulting and/or brecciation.

XIV-4. Below the facies change (cf. Pl. XIV-2) gravitational features were seen. The slumped layers here dip 43° towards the NE (65°). The overlying layers are undisturbed and no faulting zone and/or brecciation zone were found here.

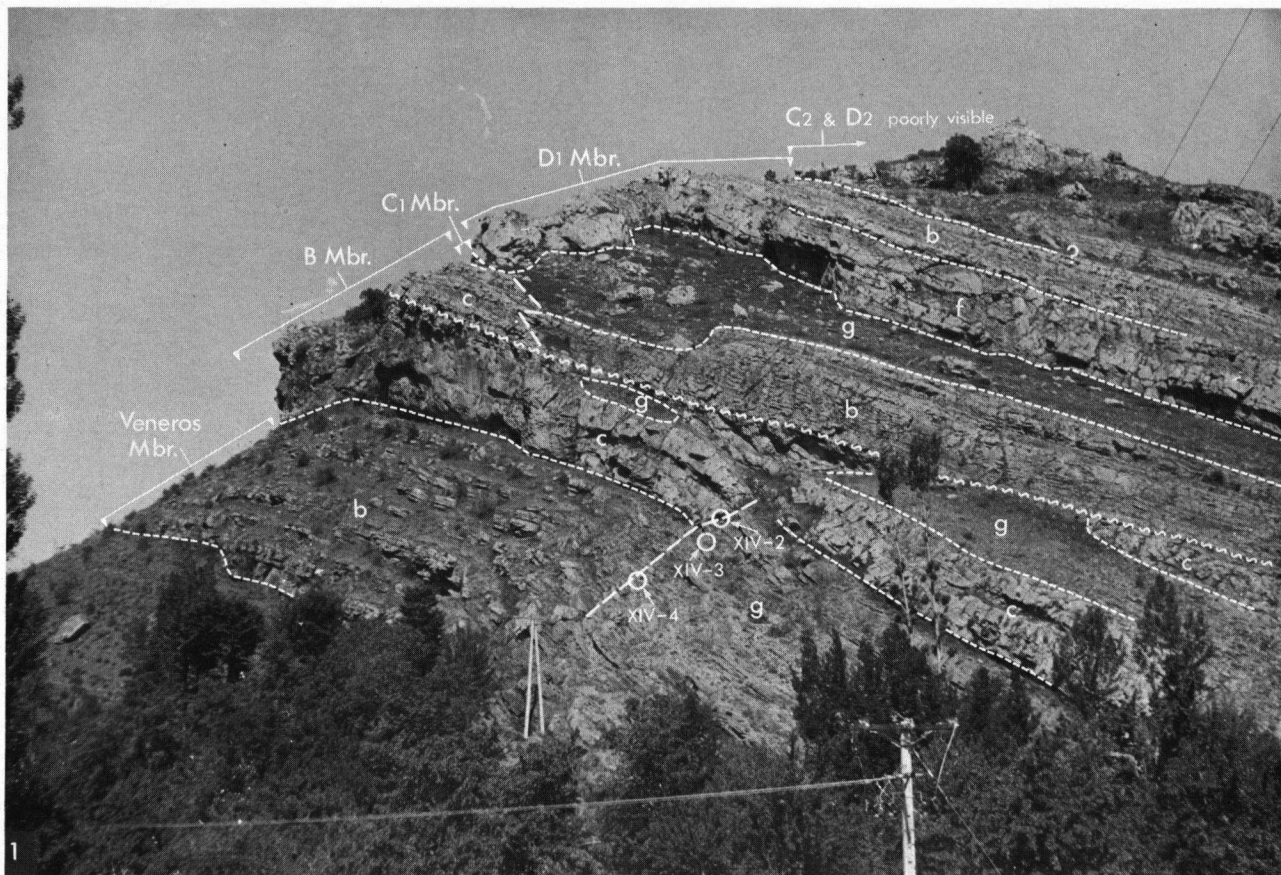


PLATE XV

XV-1. Electron photomicrograph. Section 24. Sample 558. Sample treated with CH_2ClCOOH . Residue is mainly ferruginous material. Colour is 10 R 4/6. X-ray diffractogram shows typical picture of amorphous mass. Electron microscope (Photographs by Mr. W. de Priester) shows tiny crystals by magnification of 12500. Comparison with Atlas of Electron microscopy of clay minerals and their admixtures (Beutelspacher & van der Marel, 1968) shows interesting resemblances with goethite and hematite and possibly with pyrite.

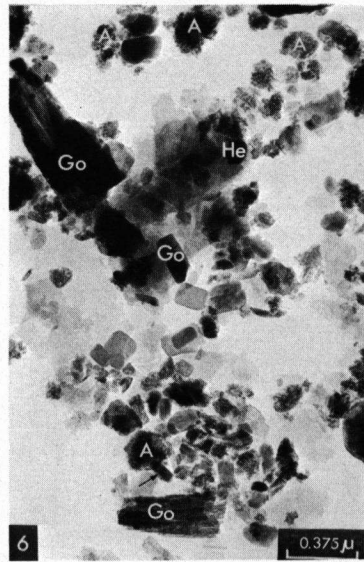
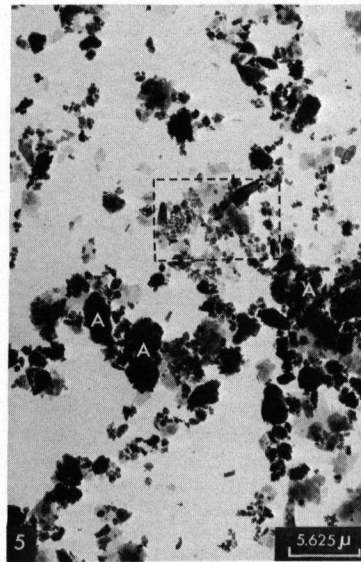
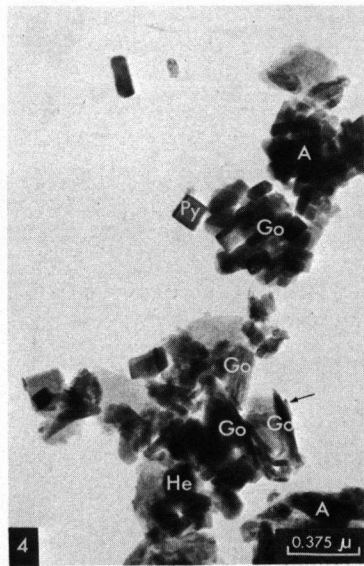
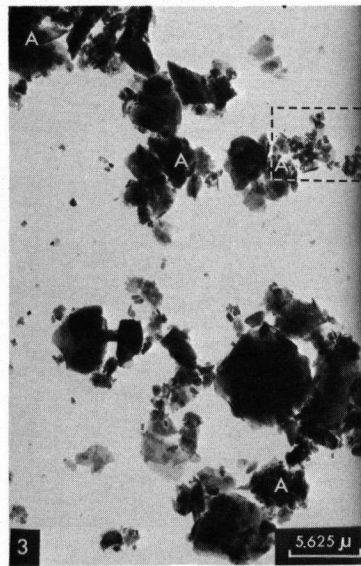
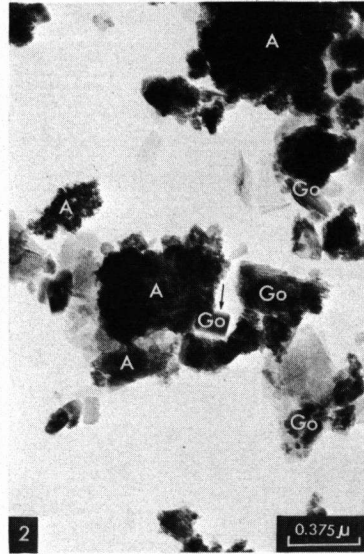
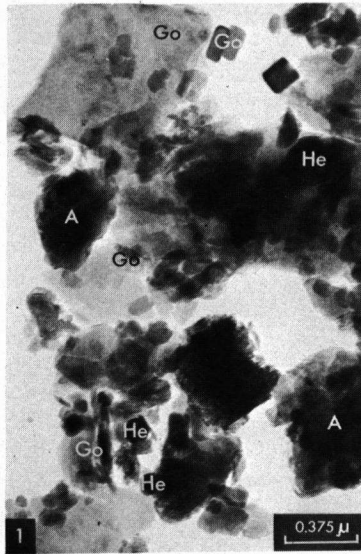
Identification of electron microscopy of iron minerals generally is hampered by a moderate to strong scattering of the electron rays which makes the particles opaque (Beutelspacher & v. d. Marel, 1968, p. 177). Hematite particles occur as small opaque grains (cf. Beutelspacher & v. d. Marel, 1968, Fig. 184-188) and many grains possess hexagonal-like angles. This is also the case in some of the here presented photographs (He). Goethite (Go) is well crystallized contrary to limonite. It is opaque and shows sometimes growth striation. Crystals are coarsely, and sometimes well developed needle-like. Prismatic crystals too can be present (cf. Beutelspacher and v. d. Marel, 1968, Fig. 171-175). A fairly important other constituent are the clotty, irregularly distributed aggregates (A). Some of these grains have an extreme fine granular substructure, and a very irregular surrounding. This strongly points towards a mobile form of the iron in the sediment (probably as a ferric hydroxide sol or gel). Authigenic dehydration of these ferric hydroxide gels may result in goethite, limonite and lepidocrocite (?), and further dehydration leads to hematite. Goethite crystallizes from a ferric hydroxide gel at high pH-values. Only under the influence of adsorbed negative ions (HCO_3^- , SO_4^{2-}) it may precipitate at neutral pH values. Hematite crystallizes at low pH values, and, under the influence of adsorbed positive ions (Mg^{2+} , Ca^{2+}), at neutral pH values.

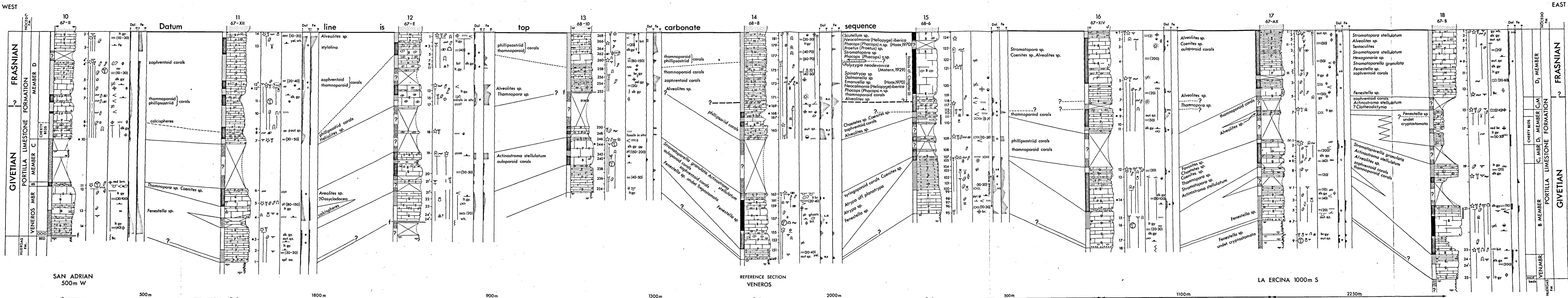
The paragenesis of amorphous clotty aggregates of iron mineral, of crystals of goethite and of crystals of hematite leads to the conclusion that pH value must have been approximately neutral and that different types of iron must have been adsorbed.

XV-2. Electron micrograph. Section 33. Sample 1. Sample treated with CH_2ClCOOH . Residue mainly ferroan material. Colour 10 YR 5/4. Moderate yellowish brown. X-ray diffractogram shows a typical picture for amorphous material but a few peaks lead to the conclusion that goethite, hematite (?) and pyrite (?), and some miscellaneous quartz is present (Mr. R. O. Feliuss, pers. comm.). For a general description cf. Pl. XV-1. The clotty irregular aggregates of iron material with the very fine grained sub-structure is clearly visible. One prismatic (goethite ?) crystal is forming out of the aggregate. Some clearly recognizable needle-like crystals of goethite (Go) are recognizable, and on some crystals, growth striae can be seen.

XV-3 and XV-4. Section 33. Sample 1. Some clotty precipitates with irregular shapes (generally amorphous) are present. Irregularly distributed extremely small crystals (50-70 Å) of a generally prismatic and occasionally cubic habit, are present. Possibly we deal here with pyrite (minor amounts), hematite (?) and goethite. The presence of the last two minerals is confirmed by X-ray analysis, and by comparison with Figs. 173, 175 of Beutelspacher & v. d. Marel, 1968.

XV-5 and XV-6. Section 24. Sample 558. Amorphous material with scattered authigenic crystals of goethite, pyrite (?) and hematite (?). Growth striae are visible in a few cases. In the clotty aggregates the extremely fine granular sub-structure is visible. A few crystals are possibly 'forming' and are 'caught' during forming.



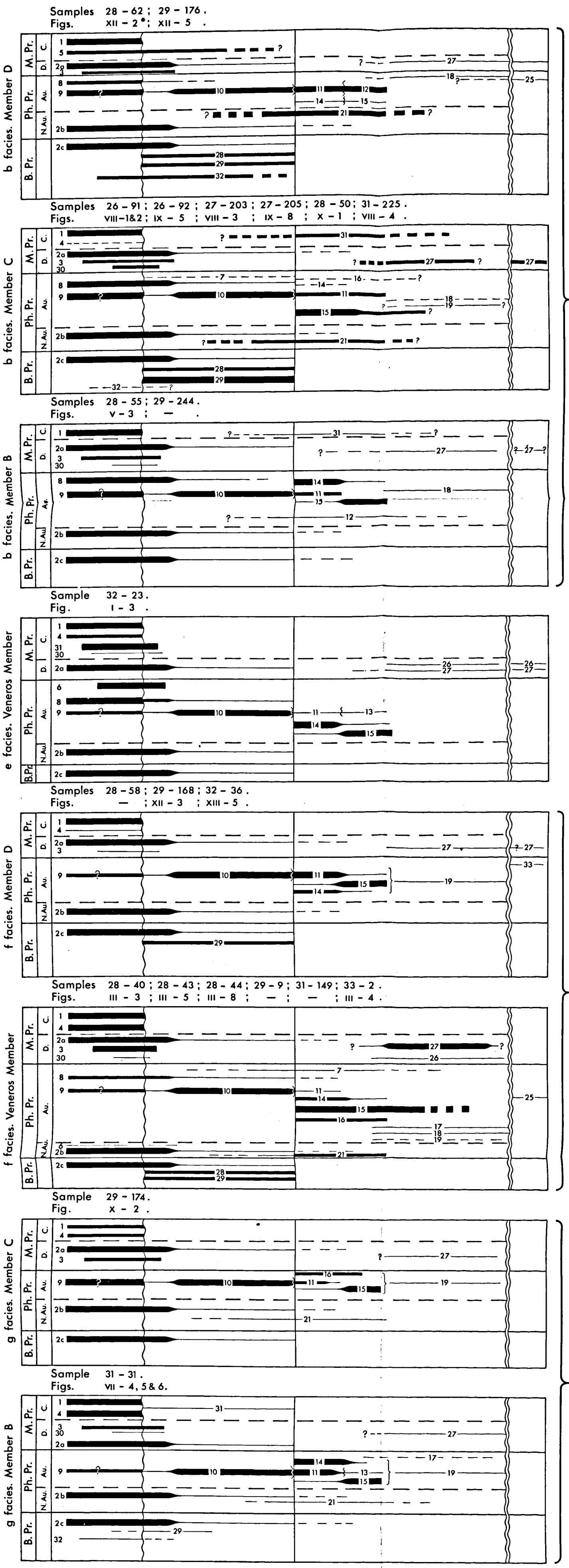


HORIZONTAL NOT TO SCALE VERTICAL SCALE 1:600

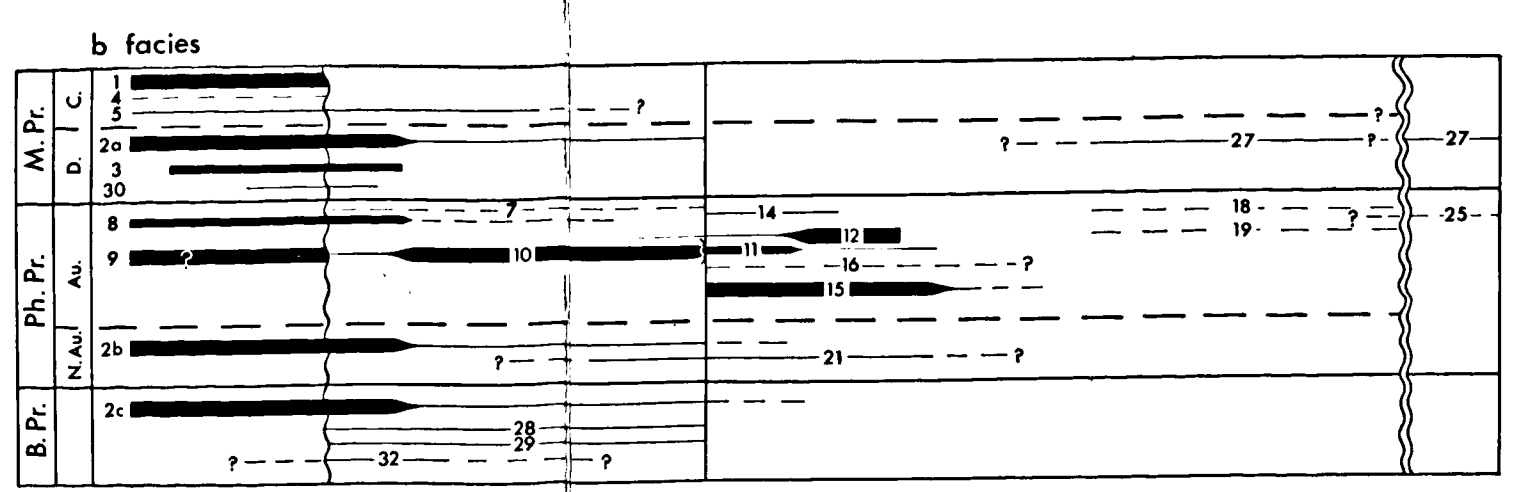
PARAGENESIS OF DIAGENETIC PROCESSES IN THE RECOGNISED FACIES, PLOTTED AGAINST RELATIVE TIME OF ACTION.

1st LEVEL

2nd LEVEL



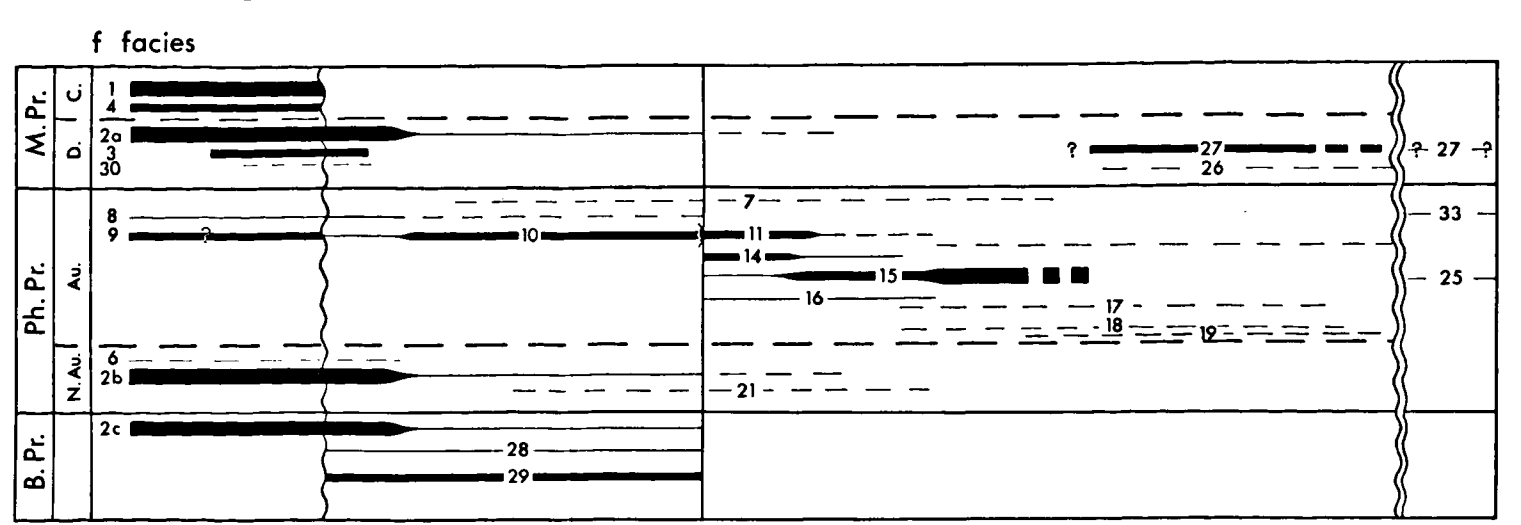
ESLA AUTOCHTHONOUS AREA



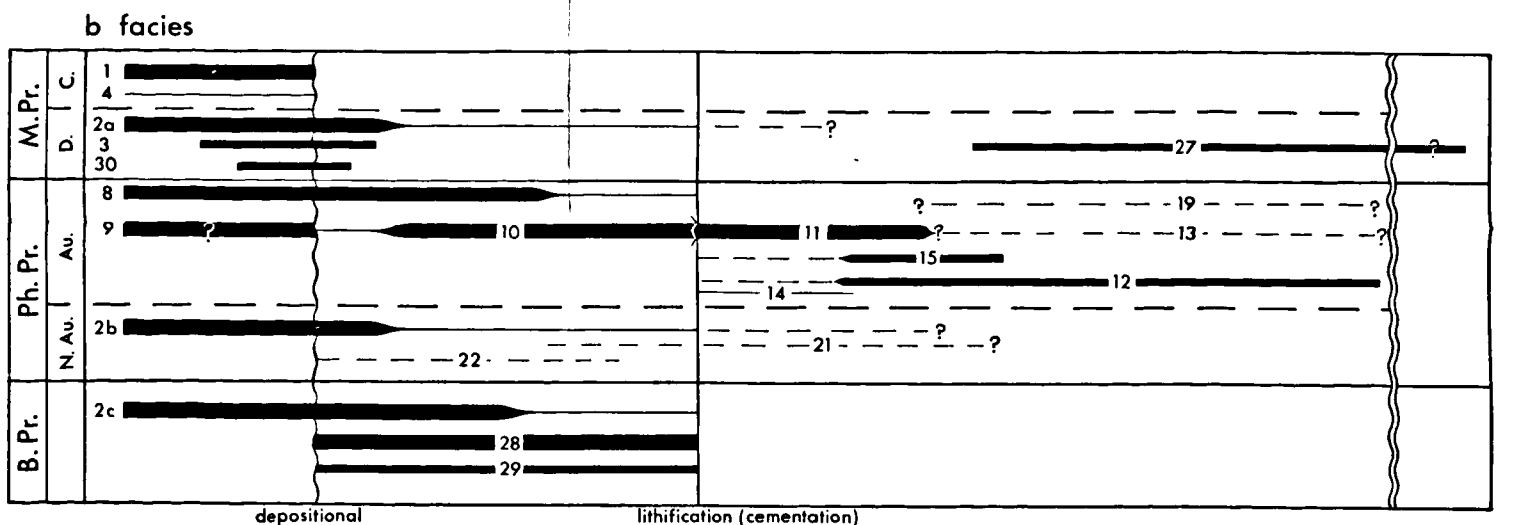
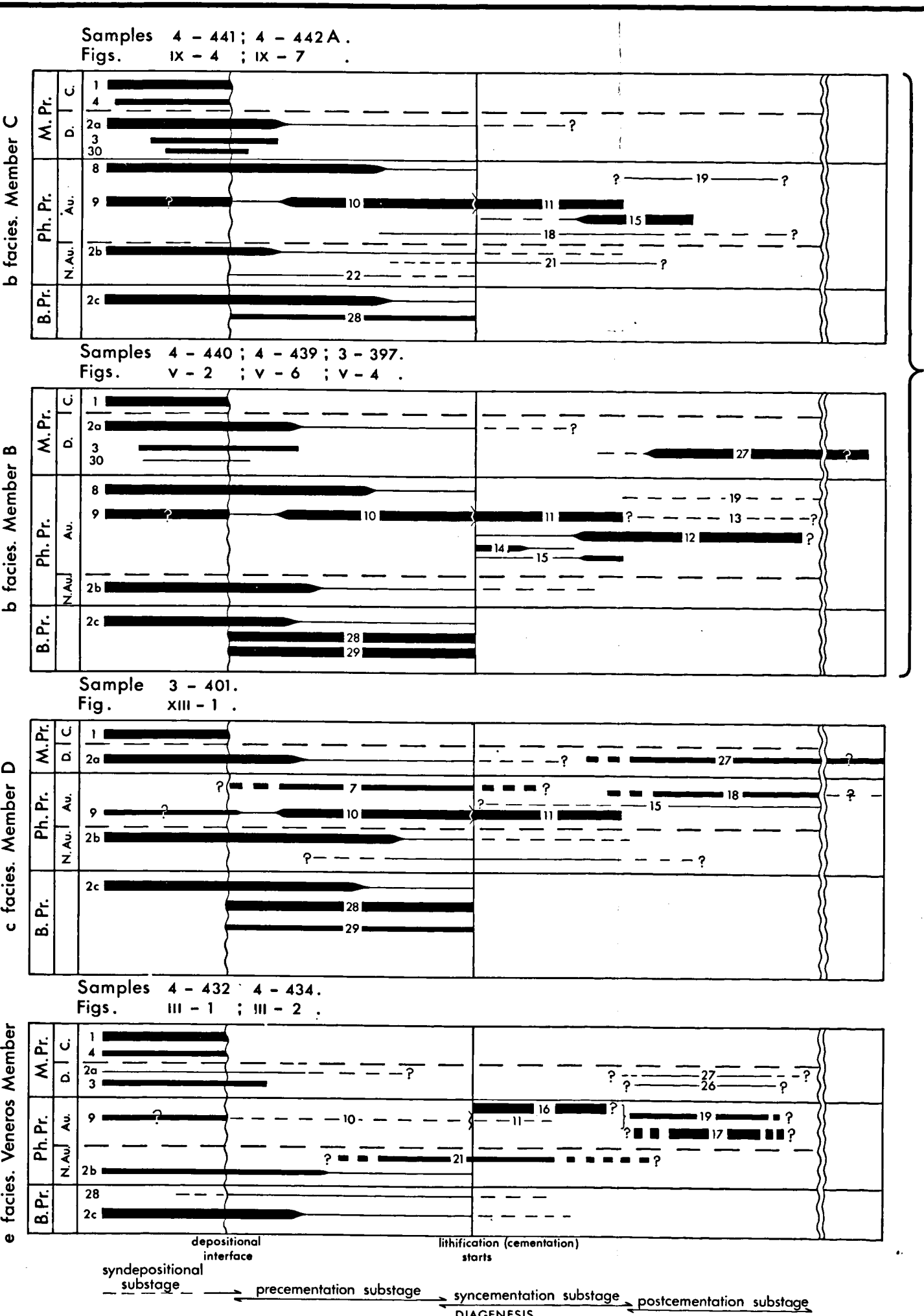
RECOGNISED PROCESSES

- | | |
|---|--|
| 1 Accumulation of bioclastic material | 16 Syntaxial rim cement & syntaxial grain growth rims |
| 2a Mechanical disintegration of carbonate material | 17 Replacement of (patchy) dolomite |
| 2b Physicochemical disintegration of carbonate material | 18 Formation of rhombohedral dolomite crystals |
| 2c Biochemical disintegration of carbonate material | 19 Recrystallisation <i>sensu lato</i> |
| 3 Washing out of accumulated carbonate material | 20 Replacements $Ca \rightleftharpoons Qz$ |
| 4 Accumulation of non-carbonate material | 21 Formation of (micro) stylolites |
| 5 Formation of limeclasts | 22 Formation of impregnations in grains |
| 6 Formation of ooids | 23 Dedolomitisation |
| 7 Precipitation of quartz and chert | 24 Expulsion of impurities |
| 8 Precipitation of ferruginous material | 25 Infilling (2 nd phase) with ferruginous material |
| 9 Direct precipitation of mud | 26 Fracturing |
| 10 Mechanical formation of mud | 27 Formation of bioturbation structures |
| 11 Formation of micrite | 28 Formation of pellets |
| 12 Formation of micro sparite | 29 Formation of voids |
| 13 Formation of pseudo sparite | 30 Mechanical infilling of open void structures |
| 14 Precipitation of fibrous cement crystals | 31 Algal coating and boring |
| 15 Precipitation of equant cement crystals | 32 Flattening of carbonate particles |

Mechanical processes	M. Pr.	Constructive processes	rarely occurring process
	D. C.	Destructive processes	
Physicochemical processes	Ph. Pr.	Authigenous processes	fairly occurring process
	N. Au. I. Au.	Non Authigenous processes	abundantly occurring process
Biochemical processes	B. Pr.	not subdivided	fairly occurring process
			uncertain
			sporadically occurring process
			rarely occurring process



PEDROSO SYNCLINE AREA



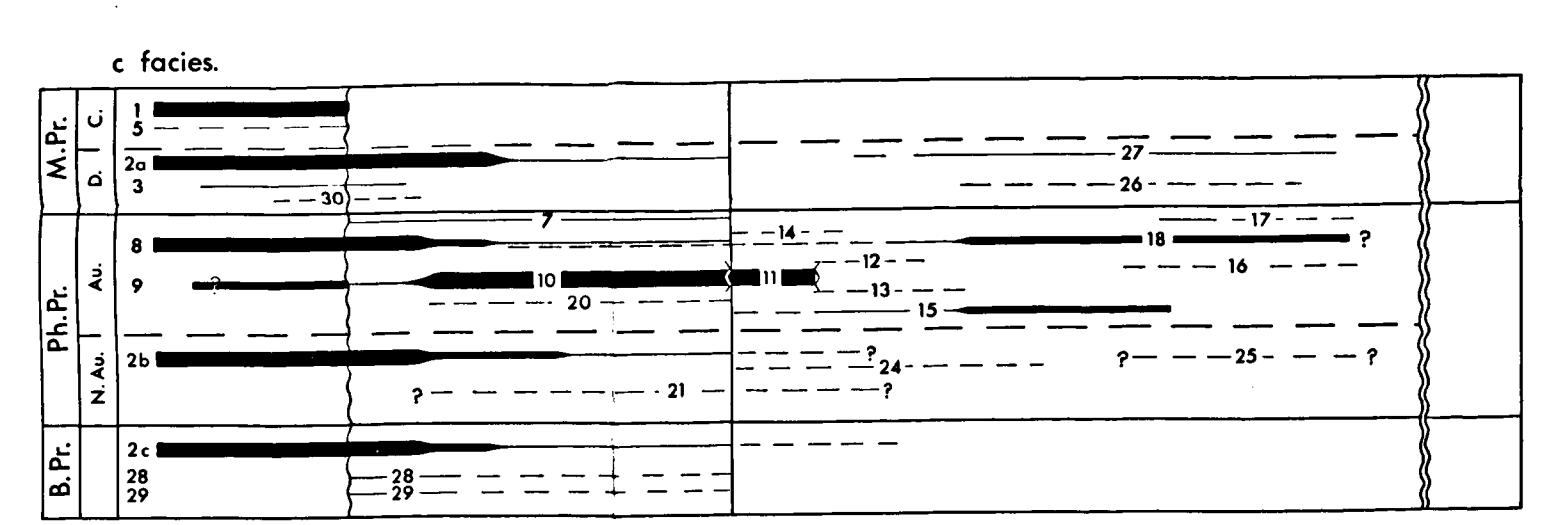
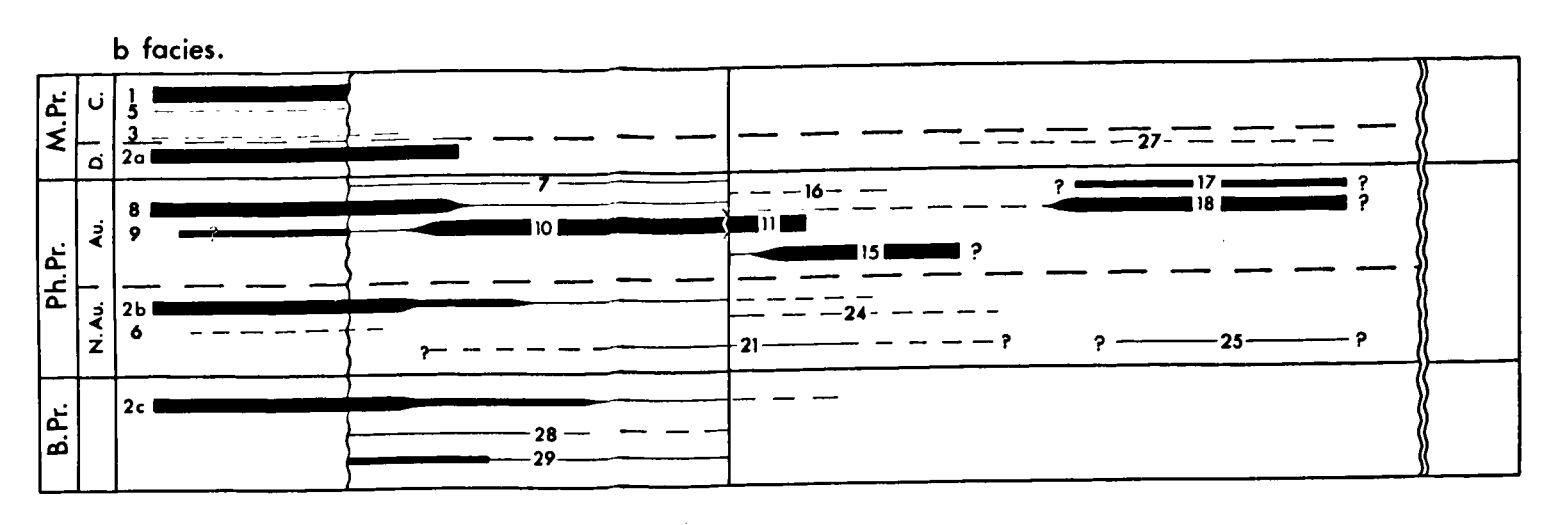
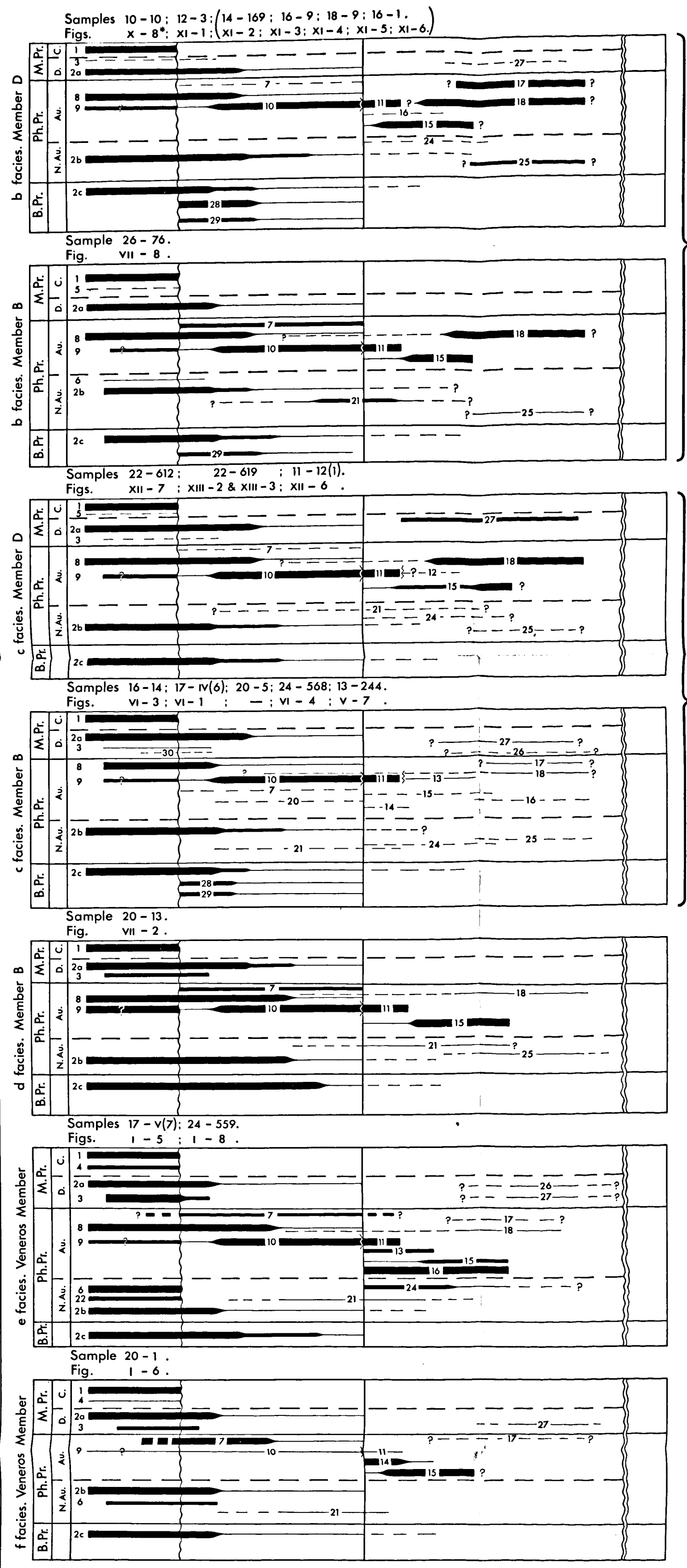
M. = Metamorphism
 * = Roman numeral refers to plate, Arabic numeral refers to photograph

PARAGENESIS OF DIAGENETIC PROCESSES IN THE RECOGNISED FACIES, PLOTTED AGAINST RELATIVE TIME OF ACTION.

1st LEVEL

2nd LEVEL

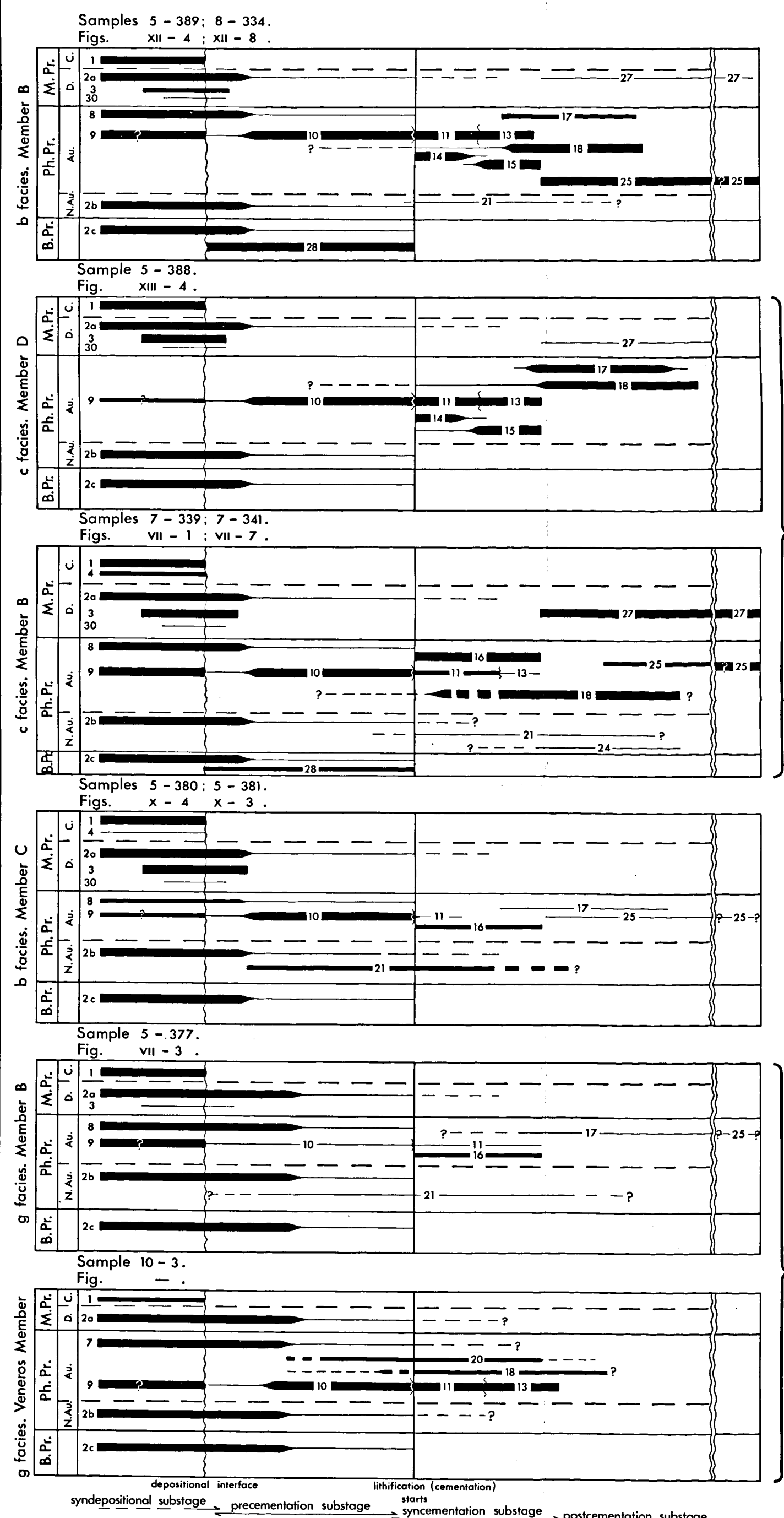
PENA CORADA AREA



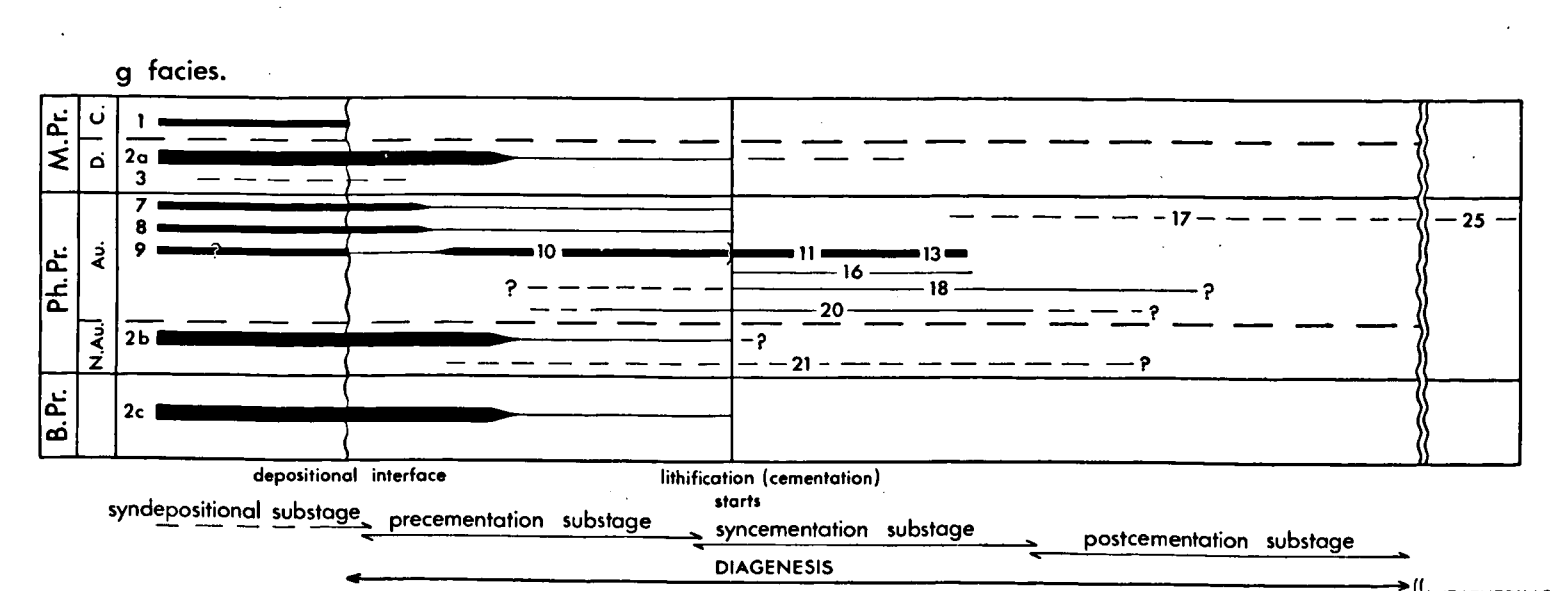
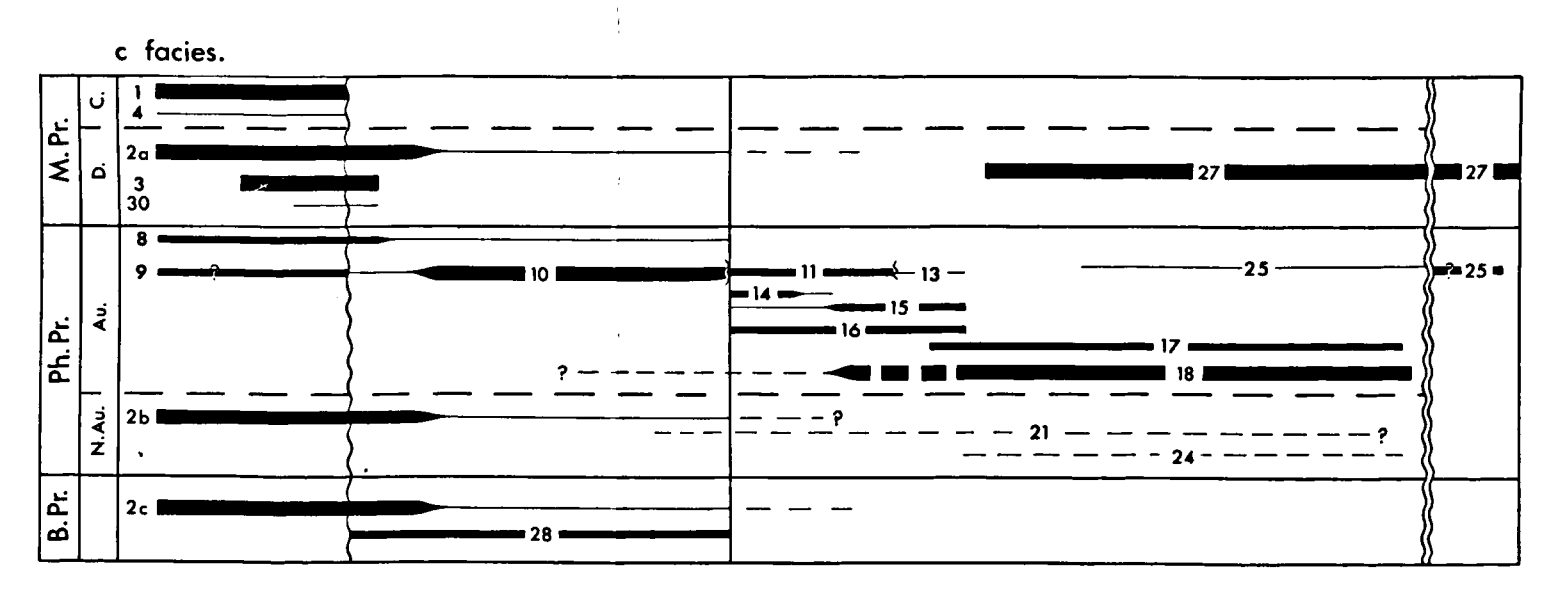
RECOGNISED PROCESSES

1	Accumulation of bioclastic material	16	Syntaxial rim cement & syntaxial grain growth rims
2a	Mechanical disintegration of carbonate material	17	Replacement of (patchy) dolomite
2b	Physicochemical disintegration of carbonate material	18	Formation of rhombohedral dolomite crystals
2c	Biochemical disintegration of carbonate material	19	Recrystallisation <i>sensu lato</i>
3	Washing out of accumulated carbonate material	20	Replacements Ca → Qz
4	Accumulation of non-carbonate material	21	Formation of (micro) stylolites
5	Formation of limeclasts	22	Formation of impregnations in grains
6	Formation of ooids	23	Expulsion of impurities
7	Precipitation of quartz and chert	24	Expulsion of impurities
8	Precipitation of ferruginous material	25	Defoliation
9	Direct precipitation of mud	26	Infilling (2 nd phase) with ferruginous material
10	Mechanical formation of mud	27	Fracturing
11	Formation of micrite	28	Formation of bioturbation structures
12	Formation of micro sparite	29	Formation of pellets
13	Formation of pseudo sparite	30	Formation of voids
14	Precipitation of fibrous cement crystals	31	Mechanical infilling of open void structures
15	Precipitation of equant cement crystals	32	Algal coating and boring
		33	Flattening of carbonate particles

Mechanical processes	M.Pr. C	Constructive processes	rarely occurring process
	D	Destructive processes	sporadically occurring process
Physicochemical processes	Ph.Pr. Au.	Authigenous processes	fairly occurring process
	N.Au.	Non Authigenous processes	abundantly occurring process
Biochemical processes	B.Pr.	not subdivided	fairly occurring process
			uncertain
			sporadically occurring process
			rarely occurring process



ALBA SYNCLINE AREA



depositional interface lithification (cementation) starts

syndepositional substage pre-cementation substage syncementation substage post-cementation substage

← DIAGENESIS →

WEATHERING

M. = Metamorphism
* = Roman numeral refers to plate, Arabic numeral refers to photograph

LEGEND TO ENCLOSURES I - IV

LITHOLOGY

- | | |
|------------------------------------|---|
| Limestone 0-10% Dol. | Limestone, containing chert nodules |
| Dolomitic limestone 10-50% Dol. | Nodular limestone |
| Calcitic dolomite 50-90% Dol. | Shale |
| Dolomite 90-100% Dol. | Marl |
| Lime mudstone | Sandstone/siltstone |
| Lime wackestone | Ooid; Superficial ooid |
| Lime packstone | Pelletoid limestone |
| Lime grainstone | Onkoid limestone, grapestone |
| Lime boundstone | Non skeletal, muddy intraclast < 4 mm & > 4mm |
| Chalky lime mudstone | Skeletal intraclast < 4mm & > 4mm |
| Much recrystallised packstone | |
| Very much recrystallised packstone | |
| Calcarenite - calcirudite > 63µ | |
| Calcisiltite - calcilutite < 63µ | |
| Breccia | |
| Marly limestone | |
| Silty limestone | |
| Shaly limestone | |

FACIES TYPES

- | | |
|--|---|
| | b |
| | c |
| | d |
| | e |
| | f |
| | g |

FOSSILS AND FOSSILFRAGMENTS

- | | |
|---|----------------|
| ☆ Crinoid | Ⓐ Algae |
| Υ Bryozoan | Ⓐ Trilobites |
| Ⓢ Encrusting bryozoan | Ⓐ Gastropod |
| Ⓞ Ostracod | ♂ Pelecypod |
| ∇ Brachiopod | Ⓐ Conodont |
| Υ Stylolina | Ⓐ Foraminifera |
| ∇ Tentaculites | Ⓐ Stromatopora |
| ☆ Calcispheres | ♣ Plants |
| ⊙ Coral (general) | Ⓜ Wood |
| Ⓢ Stick-like or rod-like (e.g. <i>Thamnopora</i> sp.) | |
| Ⓢ Platy (e.g. <i>Alveolites</i> sp.) | |
| Ⓢ Massive (e.g. <i>Chaetetes</i> sp.) | |
| Ⓢ Solitary (e.g. <i>Zaphrentoid</i>) | |
| Ⓢ Massive (e.g. <i>Heliolites</i> sp.) | |
- } Tabulate corals
} Rugose corals

SEDIMENTOLOGY

- == (10-20) Bedding thickness
- == Regular bedded
- ≈ Wavy bedded
- ▲ Solution phenomena, solution stringers, stylolites
- ⊙ Slumping features
- ∞ Pellets
- ⊕ Burrowing (general)
- ⊕ Horizontal burrows
- < Wedges
- ≪ Pronounced wedges
- ≠ Unlayered
- ≡ Grading
- ∩ Gullies
- ∩ Loading features
- ⊙ Geopetal structures (sheltering; "umbrella effect")
- ⊙ Silicified corals

ABBREVIATIONS

- a. - anhedral crystal
- aut. - autigenous crystal
- bit. - bituminous
- bl. - black
- br. - brown
- d. - disconformity
- det. - detrital
- Dol. - dolomite
- dk. - dark
- e. - euhedral crystal
- f. - fault
- Fe. - ferruginous material
- gl. - glauconite
- gr. - green
- gy. - grey
- lt. - light
- p.sol. - pressure solution
- pyr. - pyrite

GENERAL

- Much solitary corals
- Very much solitary corals
- Interval in which solitary corals occur
- Thrust fault
- Disconformity
- Lithostratigraphic correlation lines and members
- Lithologic correlation lines of beds
- Chronostratigraphic correlation lines
- Uncertain

